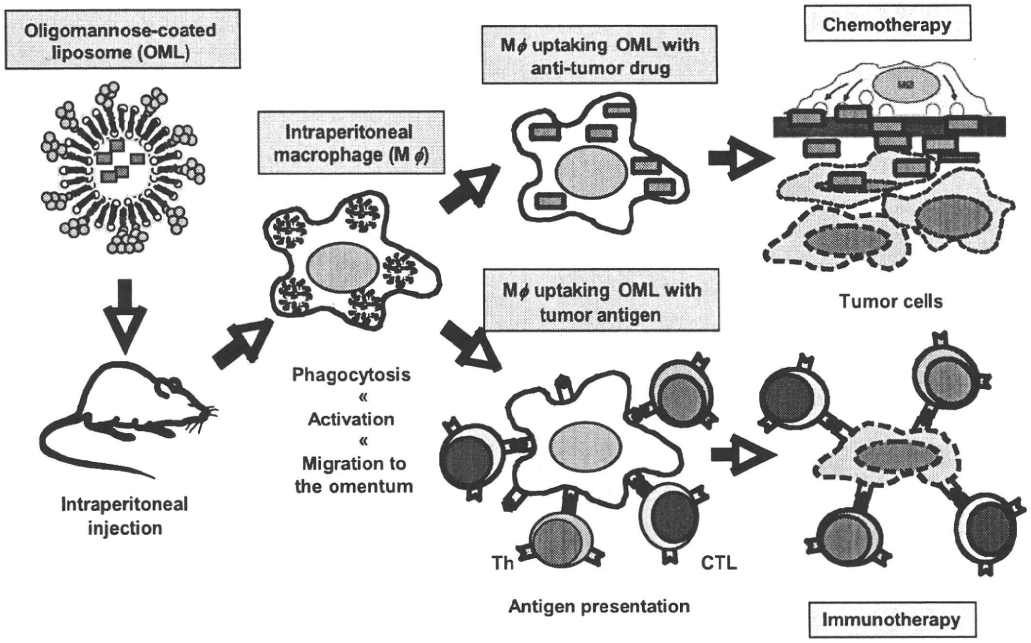

Figure 4. Applications of OMLs for tumor treatment.

OMLs are very useful not only for the promotion of antigen uptake by antigen-presenting cells but also for the enhancement of antigen processing of encased antigens. In general, endogenous and exogenous antigens are presented preferentially by MHC class I and II, respectively. OML-encased antigens, however, were effectively directed to both pathways, even when added exogenously. This advantage of OML-mediated immunization will hopefully facilitate the simultaneous activation of tumor-specific $CD4^+$ and $CD8^+$ T cells as shown in this study with OVA. In addition, intraperitoneal uptake of OMLs also induces Mϕ maturation with up-regulation of MHC class II and co-stimulatory molecules and IL-12 production, resulting in an effective induction of antigen-specific type 1 helper T cell (Th1) responses (19, 20). Indeed, OT-I and OT-II T cells stimulated with Mϕ ingesting OML-OVA produced IFN-γ but not IL-4 or IL-10 (Figure 2 and unpublished observation).

Recently, we have shown that OMLs activate phosphatidylinositol 3-kinase/Akt pathway through phosphorylation of Src family kinases to induce the activation of mitogen-activated protein kinases in Mϕ-like J774A.1 cells (21). We have also shown that peritoneal Mϕ uptake OMLs through a cooperation of specific ICAM-3 garbbing nonintegrin-related 1 (SIGNR1) and complement receptor type 3 (CR3) (22, 23). Thus, SIGNR1 (maybe together with CR3) may associate with nonreceptor-type tyrosine kinases in lipid rafts during OML recognition, and complexes of these molecules facilitate subsequent OML uptake and signal transduction to induce an OML-induced Th1 response.

In order to apply our OMLs in clinical study, the best administration routes should be determined to pursue repetitive vaccination while avoiding possible side effects. As generally acknowledged, intraperitoneal administration is accompanied with a high risk of side effects such as catheter-related complications and abdominal pain. Indeed, it is difficult to complete repetitive intraperitoneal chemotherapy in some cases due to such side effects (24). In this connection, we have already obtained effective *in vivo* anti-tumor responses by subcutaneous injection of OMLs containing tumor antigens (25). However, side effects induced by subcutaneous injection of OMLs should be further investigated to assure their safe clinical application.

In the previous study, we reported that the formation of peritoneal metastasis of seeded gastric cancer cells in milky spots can be controlled with OMLs containing anti-cancer drugs (10). In the present study, we have further extended the possibility of OMLs for the immunotherapy of systemic metastasis and existing tumor cells aside from milky spots. Oligomannose-coating of liposomes showed the best uptake efficiency by peritoneal Mϕ among the neoglycolipids so far tested, and the encased antigen was effectively presented by both MHC class I and II

molecules. However, the effects for immune responses induced by other neoglycolipids have not been studied at all so far. We have a great interest in this issue and are seeking the materials with immunoregulatory properties. If such materials would be found, our neoglycolipid-coated liposome technology might be further applicable for antigen-specific regulation of autoimmune diseases and allergy.

Acknowledgement

This work was supported by the Industrial Technology Research Grant Program of the New Energy and Industrial Technology Development Organization (NEDO) of Japan, in part by a grant for Hi-tech research program from Tokai University, and by the Program for Promotion of Basic Research Activities for Innovative Biosciences (PROBRAIN).

References

1. Gattinoni L, Powell DJ Jr, Rosenberg SA, Restifo NP. 2006. Adoptive immunotherapy for cancer: building on success. *Nat. Rev. Immunol.* 6: 383-393.
2. Rosenberg SA, Yang JC, Restifo NP. 2004. Cancer immunotherapy: moving beyond current vaccines. *Nat. Med.* 10: 909-915.
3. Rosenberg SA. 2001. Progress in the development of immunotherapy for the treatment of patients with cancer. *J. Intern. Med.* 250: 462-475.
4. Boon T, Coulie PG, Van den Eynde BJ, van der Bruggen P. 2006. Human T cell responses against melanoma. *Annu. Rev. Immunol.* 24: 175-208.
5. Pardoll DM, Topalian SL. 1998. The role of $CD4^+$ T cell responses in antitumor immunity. *Curr. Opin. Immunol.* 10: 588-594.
6. Wang RF, Peng G, Wang HY. 2006. Regulatory T cells and Toll-like receptors in tumor immunity. *Semin. Immunol.* 18: 136-142.
7. Sakaguchi S, Setoguchi R, Yagi H, Nomura T. 2006. Naturally arising Foxp3-expressing $CD25^+CD4^+$ regulatory T cells in self-tolerance and autoimmune disease. *Curr. Top. Microbiol. Immunol.* 305: 51-66.
8. Leen AM, Rooney CM, Foster AE. 2007. Improving T cell therapy for cancer. *Annu. Rev. Immunol.* 25: 243-265.
9. Ikehara Y, Kojima N. 2007. Development of a novel oligomannose-coated liposome-based anticancer drug-delivery system for intraperitoneal cancer. *Curr. Opin. Mol. Ther.* 9: 53-61.
10. Ikehara Y, Niwa T, Biao L, Ikehara SK, Ohashi N, Kobayashi T, Shimizu Y, Kojima N, Nakanishi H. 2006. A carbohydrate recognition-based drug delivery and controlled release system using intraperitoneal macrophages as a cellular vehicle. *Cancer Res.* 66: 8740-8748.
11. Krist LF, Kerremans M, Broekhuis-Fluitsma DM, Eestermans IL, Meyer S, Beelen RH. 1998. Milky spots in the greater omentum are predominant sites of local tumour cell proliferation and accumulation in the peritoneal cavity. *Cancer Immunol. Immunother.* 47: 205-212.
12. Hagiwara A, Takahashi T, Sawai K, Taniguchi H, Shimotsuma M, Okano S, Sakakura C, Tsujimoto H, Osaki K, Sasaki S, Shirasu M. 1993. Milky spots as the implantation site for malignant cells in peritoneal dissemination in mice. *Cancer Res.* 53: 687-692.
13. Hogquist KA, Jameson SC, Heath WR, Howard JL, Bevan MJ, Carbone FR. 1994. T cell receptor antagonist peptides induce positive selection. *Cell* 76: 17-27.
14. Clarke SR, Barnden M, Kurts C, Carbone FR, Miller JF, Heath WR. 2000. Characterization of the ovalbumin-specific TCR transgenic line OT-I: MHC elements for positive and negative selection. *Immunol. Cell Biol.* 78: 110-117.
15. Barnden MJ, Allison J, Heath WR, Carbone FR. 1998. Defective TCR expression in transgenic mice constructed using cDNA-based α- and β-chain genes under the control of heterologous regulatory elements. *Immunol. Cell Biol.* 76: 34-40.
16. Gorer PA. 1950. Studies in antibody response of mice to tumour inoculation. *Br. J. Cancer* 4: 372-379.
17. Moore MW, Carbone FR, Bevan MJ. 1998. Introduction of soluble protein into the class I pathway of antigen processing and presentation. *Cell* 54: 777-785.
18. Mizuochi T, Loveless RW, Lawson AM, Chai W, Lachmann PJ, Childs RA, Thiel S, Feizi T. 1989. A library of oligosaccharide probes (neoglycolipids) from N-glycosylated proteins reveals that conglutinin binds to certain complex-type as well as high mannose-type oligosaccharide chains. *J. Biol. Chem.* 264: 13834-13839.
19. Shimizu Y, Takagi H, Nakayama T, Yamakami K, Tadakuma T, Yokoyama N, Kojima N. 2007. Intraperitoneal immunization with oligomannose-coated liposome-entrapped soluble leishmanial antigen induces antigen-specific T-helper type 1 immune response in BALB/c mice through uptake by peritoneal macrophages. *Parasite Immunol.* 29: 229-239.
20. Takagi H, Furuya N, Kojima N. 2007. Preferential production of IL-12 by peritoneal macrophages activated by liposomes prepared from neoglycolipids containing oligomannose residues. *Cytokine* 40: 241-250.

21. Kato C, Kajiwara T, Numazaki M, Takagi H, Kojima N. 2008. Oligomannose-coated liposomes activate ERK via Src kinases and PI3K/Akt in J774A.1 cells. *Biochem. Biophys. Res. Commun.* 372: 898-901.
22. Abe Y, Kuroda Y, Kuboki N, Matsushita M, Yokoyama N, Kojima N. 2008. Contribution of complement component C3 and complement receptor type 3 to carbohydrate-dependent uptake of oligomannose-coated liposomes by peritoneal macrophages. *J. Biochem.* 144: 563-570.
23. Takagi H, Numazaki M, Kajiwara T, Abe Y, Ishii M, Kato C, Kojima N. 2009. Cooperation of specific ICAM-3 grabbing nonintegrin-related 1 (SIGNR1) and complement receptor type 3 (CR3) in the uptake of oligomannose-coated liposomes by macrophages. *Glycobiology* 19: 258-266.
24. Armstrong DK, Bundy B, Wenzel L, Huang HQ, Baergen R, Lele S, Copeland LJ Walker JL, Burger RA, Gynecologic Oncology Group. 2006. Intraperitoneal cisplatin and paclitaxel in ovarian cancer. *N. Engl. J. Med.* 354: 34-43.
25. Kojima N, Biao L, Nakayama T, Ishii M, Ikehara Y, Tsujimura K. 2008. Oligomannose-coated liposomes as a therapeutic antigen-delivery and an adjuvant vehicle for induction of in vivo tumor immunity. *J. Control. Release* 129: 26-32.

Mucosal Vaccine Using CTL Epitope-Pulsed Dendritic Cell Confers Protection for Intracellular Pathogen

Yuichi Ozawa[1], Takafumi Suda[1], Toshi Nagata[2], Dai Hashimoto[1], Yutaro Nakamura[1], Noriyuki Enomoto[1], Naoki Inui[1,3], Yukio Koide[2], Hirotoshi Nakamura[1], and Kingo Chida[1]

[1]Second Division, Department of Internal Medicine, [2]Department of Microbiology and Immunology, and [3]Department of Clinical Pharmacology and Therapeutics, Hamamatsu University School of Medicine, Hamamatsu, Japan

Effective protective immunity against respiratory infections with intracellular pathogens requires pathogen-specific cytotoxic T cells (CTL) in the lung. However, vaccines that induce pathogen-specific CTL in the lung are poorly explored. Dendritic cells (DC) have increasingly been exploited as vaccines against infections. However, few studies have investigated the ability of mucosal DC vaccines to elicit protective CTL responses in the lung. Our objective was to develop an efficacious mucosal DC vaccine to generate protective CTL against respiratory infections with intracellular pathogens. Bone marrow–derived DC (BM-DC) pulsed with a single immunodominant CTL epitope, listeriolysin O (LLO) 91-99, of *Listeria monocytogenes* (LM) were intratracheally administered into mice. The frequency and function of epitope-specific CTL in mediastinal lymph nodes (MLN) and spleen were assessed for their ability to protect against LM infection. After intratracheal administration, lipopolysaccharide (LPS)-treated LLO 91-99–loaded BM-DC (LPS-LLO DC) more frequently migrated to MLN than LPS-untreated LLO 91-99–loaded BM-DC (LLO DC). Using tetrameric H2-K^d/LLO 91-99 peptide complex, specific CD8$^+$ T cells were found in MLN as well as the spleen in LPS-LLO DC–immunized mice, but not in LLO-DC–immunized mice. Both MLN and spleen cells obtained from LPS-LLO DC–immunized mice produced large amounts of IFN-γ in response to LLO 91-99 with high epitope-specific CTL activities. Vaccination with LPS-LLO DC, but not LLO DC, protected mice against lethal respiratory infection with LM. These data suggest that mucosal vaccination with LPS-treated immunodominant CTL epitope-loaded DC is a promising strategy for generating protective CTL against respiratory infections with intracellular pathogens.

Keywords: mucosal vaccine; *Listeria monocytogenes*; cytotoxic T cells; immunodominant epitope

Infections with intracellular pathogens, such as *Mycobacterium tuberculosis*, are a major health threat, especially in developing countries, and currently one of the most important causes of infectious death after human immunodeficiency virus infections (1). Efficient protection against intracellular pathogens is critically dependent on the induction of cellular immunity, including pathogen-specific cytotoxic T cell (CTL) responses (2). Since administration of soluble proteins is insufficient to stimulate such immunity, only live attenuated vaccines have been considered to be satisfactory to date. However, owing to the low safety of live vaccines in immunocompromised individuals and their inconsistent effectiveness, the development of new and improved vaccines against intracellular pathogens has become a current research priority. In this context, we have developed dendritic cell (DC)-based vaccines against intracellular pathogens, including *M. tuberculosis* and *Listeria monocytogenes*. We previously showed that DC vaccines genetically engineered to express protective antigens or immunodominant CTL epitopes derived from intracellular pathogens induced protective immunity against systemic infections with *M. tuberculosis* and *L. monocytogenes* in mice (3–5), and that α-galactoceramide, a ligand of natural killer T cells, boosted the effectiveness of these DC vaccines (6). However, the potential of DC as a vaccine against respiratory infections with intracellular pathogens has not been extensively explored.

CLINICAL RELEVANCE

This study showed that intratracheal injection of single immunodominant epitope-loaded dendritic cell (DC) confers protection against respiratory infections with intracellular pathogens. Thus, mucosal vaccination using cytotoxic T cell (CTL) epitope-loaded DC is a promising strategy for generating protective CTL against intracellular pathogens in the lung.

In respiratory infections with intracellular pathogens, most pathogens enter the body at the mucosal surface of the lung. Therefore, the mucosal immune system of the lung provides the first-line defense against such infections. In general, protective mucosal immune responses are most efficiently provoked by mucosal immunization. Thus, mucosal vaccination has advantages because it offers effective protection against entry of bacteria before establishment of a primary infection (1) and can stimulate both local and systemic immunity (7). Therefore, mucosal immunization of DC into the airway could be a promising candidate for a vaccine strategy against respiratory infections (8–13). Although previous studies, including ours, have shown that DC in the lung are involved in a variety of immunologic processes through their potent antigen-presenting capacity (14–17), the microenvironment in the lung biases DC-induced immune responses toward the Th2 phenotype. Indeed, intratracheally administered bone marrow–derived DC (BM-DC) were found to be prone to elicit Th2-dominated responses (18–20). To date, however, few studies have investigated the capacity of DC introduced intratracheally to elicit protective CTL responses against intracellular pathogens in the lung.

L. monocytogenes is a gram-positive intracellular bacterium that causes life-threatening infections during pregnancy and in immunocompromised individuals. Protective immunity against *L. monocytogenes* is largely mediated by CTL responses. Among the bacterially derived epitopes recognized by CTL, listeriolysin O (LLO) 91-99 is the most immunodominant epitope presented by major histocompatibility class (MHC) I H2-K^d molecules. Indeed, our previous study demonstrated that DNA immunization with a minigene plasmid encoding the single immunodominant CTL epitope LLO 91-99 induced strong CTL activity and

(*Received in original form November 19, 2008 and in final form December 19, 2008*)

This work was supported by a grant-in-aid for scientific research (13670595 to T.S.) from the Japan Society for the Promotion of Science.

Correspondence and requests for reprints should be addressed to Takafumi Suda, M.D., Ph.D., 1-20-1 Handayama, Hamamatsu, 431-3192, Japan. E-mail: suda@hama-med.ac.jp

Am J Respir Cell Mol Biol Vol 41. pp 440–448, 2009
Originally Published in Press as DOI: 10.1165/rcmb.2008-0446OC on February 6, 2009
Internet address: www.atsjournals.org

conferred partial protection against systemic infection with *L. monocytogenes* in BALB/c mice (21). Thus murine models of *L. monocytogenes* infection can serve as useful tools for studying mucosal CTL generation and protective immunity against intracellular pathogens.

The present study was conducted to develop an efficacious mucosal DC vaccine for CTL generation against respiratory infections with intracellular pathogens. To this end, we intratracheally inoculated lipopolysaccharide (LPS)-modified DC pulsed with LLO 91-99 as a single immunodominant CTL epitope of *L. monocytogenes*, and examined the ability of this DC vaccine to generate functional epitope-specific CTL and elicit protective immunity against respiratory infection with *L. monocytogenes*.

MATERIALS AND METHODS

Mice

Experiments were performed on 7- to 10-week-old male BALB/c mice (Nippon SLC, Shizuoka, Japan) and GFP-transgenic (GFP-Tg) mice on a BALB/c background. All animal experiments were performed according to the animal care guidelines of Hamamatsu University School of Medicine.

DC Preparation and Immunization

BM-DC were cultured using methods described in our previous studies (3, 5, 6). Briefly, murine BM cells were harvested from femurs and tibias of killed mice and after lysis of contaminating erythrocytes in 0.83 M NH_4Cl buffer. BM cells were cultured at 2×10^5 cells/ml in 24-well plates in RPMI 1640 supplemented with 10% fetal calf serum (FCS), 50 μM 2-mercaptoethanol, 50 μg/ml gentamicin, 1,000 U/ml of recombinant murine granulocyte-macrophage colony-stimulating factor (R&D Systems, Minneapolis, MN), and 1,000 U/ml of recombinant murine IL-4 (R&D Systems). BM-DC that had been treated with LPS (250 ng/ml; Sigma-Aldrich, St. Louis, MO) or left untreated at 1×10^6 cells/ml for 16 hours were cultured in the presence of LLO 91-99 peptide (5 μM) (GYKDGNEYI; synthesized by Invitrogen, Carlsbad, CA) and human β2-microglobulin (Chemicon International, Temecula, CA) for 1 hour. After three washes in phosphate-buffered saline (PBS), LLO 91-99–pulsed BM-DC were administered intratracheally at 2×10^6 cells/50 μl of sterile PBS.

Intratracheal Administration

Mice were anesthetized by intraperitoneal administration of 0.075 mg ketamine/0.015 mg xylazine per gram body weight. Intratracheal administration of 2×10^6 cells in 50 μl of sterile PBS was performed by infusion through the vocal cords using a fiberoptic light source (LG-PS2; Olympus Optical, Tokyo, Japan) to illuminate the entrance to the trachea.

Flow Cytometry

To assess DC migration to mediastinal lymph nodes (MLN), DC derived from GFP-Tg mice (GFP-Tg DC) with or without LPS stimulation were injected intratracheally into naive BALB/c mice. The frequencies of GFP-positive cells were analyzed with an EPICS XL flow cytometer (Beckman Coulter, Fullerton, CA). To enumerate LLO 91-99–specific $CD8^+$ T cells, a phycoerythrin (PE)-conjugated tetrameric H2-K^d/LLO 91-99 peptide complex was synthesized by MBL (Nagoya, Japan). Splenocytes and MLN cells from immunized mice were stained with the tetrameric complex and a fluorescein isothiocyanate–conjugated anti-CD8α monoclonal antibody (BD PharMingen, San Diego, CA), and analyzed using the flow cytometer.

Measurement of Cytokine Production

Splenocyte or MLN cell suspensions (2×10^6 cells/ml) obtained from immunized mice were cultured in the presence of 1 μM LLO 91-99 peptide. The supernatants were harvested after 3 days, and the levels of cytokines (IL-4, IL-5, IL-10, IL-13, and IFN-γ) were measured using a mouse cytometric bead array (BD PharMingen) according to the manufacturer's protocol.

Real-Time Reverse Transcription-Polymerase Chain Reaction Assay

After treatment of BM-DC with LPS (250 ng/ml), total RNA was isolated using an RNeasy Kit (Qiagen, Hilden, Germany) according to the manufacturer's instructions. cDNAs were generated from 2 μg of total RNA using random hexamers and an Omniscript Reverse Transcriptase Kit (Qiagen). The PCR conditions were 50°C for 2 minutes and 95°C for 10 minutes, followed by 40 cycles of 95°C for 15 seconds and 62°C for 1 minute. The primers and probes used for amplification of CCR5, CCR6, CCR7, and glyceraldehyde 3-phosphate dehydrogenase (GAPDH) were obtained from Applied Biosystems (Foster City, CA) (Assay IDs: Mm01216171 m1, Mm99999114 s1, Mm01301785 m1, and Mm99999915 g1, respectively). PCR amplification of the housekeeping gene GAPDH was performed to control for sample loading and to allow normalization among samples. Data were obtained as the relative expression levels between chemokine transcript levels and GAPDH transcript levels with STEP ONE (Applied Biosystems), and expressed as ratios to the baseline value (time 0) at each time point.

CTL Assay

For *in vitro* stimulation, splenocytes and MLN cells from immunized mice at 2 weeks after immunization were cocultured in 24-well plates at 4×10^6 cells/ml for 5 days with syngeneic splenocytes (2×10^6 cells/ml) that had been treated with 50 μg/ml mitomycin C (Roche Diagnostics GmbH, Mannheim, Germany) and pulsed with 5 μM LLO 91-99 peptide for 1.5 hours. Each well also received 10 U/ml of human recombinant IL-2 (R&D Systems). After collection of viable effector cells, varying numbers of effector cells were co-cultured with J774 cells pulsed with LLO 91-99 peptide (5 μM), comprising the target cells in this study, at 1×10^4 cells/well for 5 hour. The cell-mediated cytotoxicity specific for LLO 91-99 peptide was measured using a lactate dehydrogenase (LDH) cytotoxicity detection kit (Roche Diagnostics). The LDH released into the medium was measured and the level of specific lysis of the target cells was calculated as 100 × ([experimental release] − [spontaneous release]) / ([maximal release] − [spontaneous release]) according to the manufacturer's instructions. Spontaneous or maximal release was determined in the presence of medium alone or 1% Triton X-100, respectively.

Respiratory Infection with *L. monocytogenes* and Evaluation of Protective Immunity

L. monocytogenes strain EGD (kindly provided by M. Mitsuyama, Kyoto University, Kyoto, Japan) was maintained in brain heart infusion (BHI) broth containing 20% glycerol at −80°C until use. Before injection into mice, bacteria were grown in BHI broth overnight at 37°C with shaking until mid-log phase growth was reached. Next, *L. monocytogenes* were centrifuged into a pellet at $1{,}710 \times g$ for 15 minutes and washed twice with sterile PBS. The optical density of the bacterial suspension was determined by spectrophotometry at 600 nm. The intended number of colony-forming units (CFU) was extrapolated from a standard growth curve, and appropriate dilutions with sterile PBS were made to prepare the inoculum for the mice. The number of CFU was determined by plating 10-fold serial dilutions of the inoculum on BHI agar plates. After incubation at 37°C for 24 hours, colonies were then counted. Total CFU was calculated by multiplying the counted colony number by diluted ratio. At 2 weeks after immunization, the immunized mice were challenged intratracheally with 2.5×10^4 CFU of *L. monocytogenes* strain EGD. All animals were monitored daily for 14 days after the challenge infection. In some experiments, the mice were killed at 3 days after the challenge infection, and the numbers of bacteria in their lungs, spleens, and livers were determined by plating 10-fold dilutions of tissue homogenates on trypticase soy agar plates (BD PharMingen).

Lung Histology

For histopathologic examination, lungs were fixed in 10% formalin overnight and embedded in paraffin. Tissue sections (5 μm) were stained with hematoxylin and eosin and photographed under a microscope (VANOX; Olympus Corporation, Tokyo, Japan) using a CCD camera (DP20; Olympus Corporation).

Statistical Analysis

Data from multiple experiments were expressed as the mean ± SEM. Statistical evaluation of differences between means for experimental groups was performed by the Mann-Whitney U test and log-rank test on Kaplan-Meier survival curves using StatView-J 5.0 (SAS Institute Inc., Cary, NC). All tests were two-sided and performed at the 0.05 significance level.

RESULTS

Injected DC Migrate to Draining Lymph Nodes More Frequently when Stimulated by LPS, Together with an Increase in CCR7 mRNA Expression

Previous studies showed that intratracheally injected antigen-loaded BM-DC can migrate to MLN, where they generate antigen-specific Th2 responses (22–24). Thus, we first examined the migratory capacity of intratracheally injected DC using BM-DC obtained from GFP-Tg mice (GFP-Tg DC). As shown in Figures 1A and 1B, small numbers of GFP-Tg DC were detected in MLN at 36 hours after injection. When GFP-Tg DC were stimulated with LPS before injection, the numbers of migrating GFP-Tg DC were markedly increased (Figures 1A and 1B). No GFP-Tg DC were found in the spleen at 36 hours after injection. Chemokine receptors play major roles in mobilizing DC, and among these, chemokine receptor 7 (CCR7) is recognized as essential for DC mobilization to draining lymph nodes based on the fact that BM-DC from CCR7-deficient mice fail to migrate to draining lymph nodes (25–27). Thus, we examined the effects of LPS treatment on the mRNA expression levels of chemokine receptors in BM-DC by real-time PCR. The expression of CCR5 and CCR6 was markedly decreased, even at 6 hours after LPS exposure, while CCR7 expression was strikingly up-regulated until 12 hours (Figure 2). Since CCR5 and CCR6 are considered to be associated with DC localization to the lung (28–30), the increase in DC migration to MLN induced by LPS pretreatment is partly associated with the enhanced CCR7 expression together with the decreases in CCR5 and CCR6 expressions.

DC Immunization Induces LLO 91-99–Specific $CD8^+$ T Cells in MLN and the Spleen

We further determined the ability of intratracheal immunization with epitope-pulsed DC to induce epitope-specific $CD8^+$ T cells in MLN and the spleen. Using an LLO 91-99 peptide-specific H2-K^d tetramer, we evaluated the frequencies of tetramer-bound $CD8^+$ T cells by flow cytometry at 2 weeks after immunization. Injection of LLO 91-99 epitope-pulsed DC that had been treated with LPS (LPS-LLO DC) resulted in significantly higher occurrences of LLO 91-99–specific $CD8^+$ cells in MLN, whereas LLO 91-99 epitope-pulsed DC that had not been treated with LPS (LLO DC) induced very low frequencies of peptide-specific $CD8^+$ cells (Figure 3). LPS-treated DC without the epitope (LPS-control DC) or LPS-untreated DC without the epitope (control DC) induced virtually no LLO 91-99–specific $CD8^+$ cells in MLN or the spleen. Interestingly, intratracheal immunization with LPS-LLO DC generated similar frequencies of peptide-specific $CD8^+$ T cells in the spleen and MLN (Figure 3B).

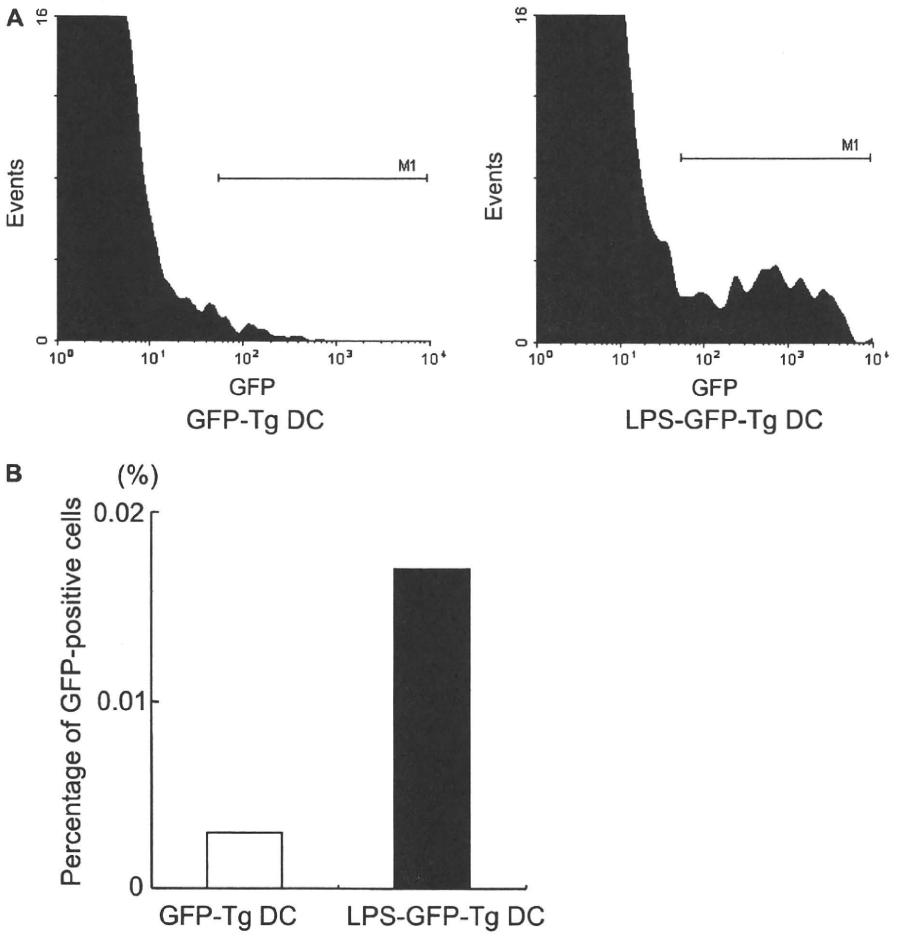

Figure 1. Effects of lipopolysaccharide (LPS) treatment on migration of intratracheally injected bone marrow–derived dendritic cells (BM-DC) to mediastinal lymph nodes. DC derived from the bone marrow of GFP-Tg mice that had been left untreated (GFP-Tg DC) or treated with LPS for 16 hours (LPS-GFP-Tg DC) were injected intratracheally into BALB/c mice at 4×10^6 cells/mice ($n = 4$ per group). (*A*) After 36 hours, mediastinal lymph nodes from each group were isolated, pooled, and analyzed by flow cytometry for migration. (*B*) Percentages of GFP-positive cells in region M1. Data are representative from two experiments.

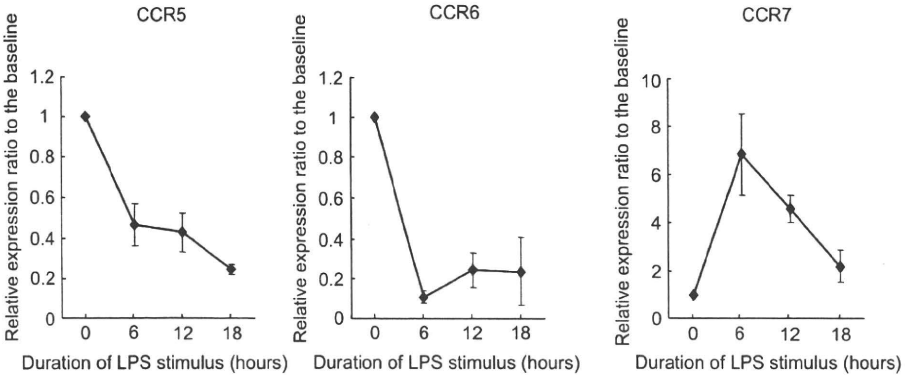

Figure 2. Effects of LPS treatment on the mRNA expression levels of chemokine receptors in BM-DC. BM-DC were stimulated with LPS (250 ng/ml), and harvested after 6, 12, and 18 hours. The mRNA expression levels were assessed by quantitative real-time PCR and the mRNA expression levels relative to the GAPDH mRNA expression levels were determined. Expression ratios relative to the corresponding baseline level (before LPS treatment) are displayed for each receptor over time. Values are expressed as the mean ± SEM of four experiments.

Previous studies have indicated that intratracheal immunization with antigen- or peptide-loaded DC, even without LPS treatment, can successfully elicit potent Th2-dominated immunity in the lung (22, 31). However, our results indicate that LPS-untreated epitope-pulsed DC did not efficiently generate peptide-specific $CD8^+$ T cells, thereby suggesting that LPS treatment is essential for the generation of such cells.

IFN-γ Production Increases in MLN and the Spleen in DC-Immunized Mice

Next, we harvested MLN and spleens from immunized mice at 2 weeks after immunization. Cells obtained from these tissues were cultured with LLO 91-99 peptide for 3 days, and the levels of cytokines in the culture supernatants were measured. In LPS-LLO DC–immunized mice, large amounts of IFN-γ were detected in both MLN and the spleen, and the amounts were significantly higher than those in LLO DC–immunized mice (Figure 4). MLN cells, but not splenocytes, from LPS-LLO DC–immunized mice also produced significantly higher levels of Th2 cytokines, including IL-4, IL-5, IL-10, and IL-13, compared with LLO DC–immunized mice (Figure 4). Collectively, these results indicate that LPS pretreatment of DC enhanced Th1 cytokine production in both MLN and the spleen, and also increased Th2 cytokine production in MLN, but not the spleen.

DC Immunization Generates Epitope-Specific CTL Activities in MLN and the Spleen

To investigate the generation of LLO 91-99–specific CTL activity in immunized mice, we measured epitope-specific cytotoxicities in MLN and the spleen using an LDH release assay with LLO 91-99–pulsed J774 cells as the target cells. At 5 days after *in vitro* stimulation, MLN and spleen cells from immunized mice were cocultured with the target cells, and the levels of LDH release were quantified. The calculated epitope-specific cytotoxicity of MLN cells was markedly higher in LPS-LLO DC–immunized mice than in LLO DC–, LPS-control DC–, and control DC–immunized mice (Figure 5). In addition, high epitope-specific cytotoxicity was observed in spleen cells from LPS-LLO DC–immunized mice, which was comparable to that in MLN cells (Figure 5). No significant differences in the epitope-specific CTL activities were found among LLO DC–, LPS-control DC–, and control DC–immunized mice. Collectively, immunization with LPS-LLO DC, but not LLO DC, efficiently generated LLO 91-99–specific CTL activities in MLN and the spleen.

DC Immunization Confers Protective Immunity against Lethal Respiratory Infection with *L. monocytogenes*

Finally, we explored whether intratracheal injection of DC can provide efficient protective immunity against lethal respiratory infection with *L. monocytogenes*. Immunized mice were challenged intratracheally with *L. monocytogenes*, and the levels of protection were assessed in two ways: namely, quantification of the numbers of *L. monocytogenes* cells recovered from organs and evaluation of survival. In our model of lethal respiratory infection with *L. monocytogenes*, the intratracheal inoculated dose was determined as 2.5×10^4 CFU, which was equal to 5-fold the dose required to kill 50% of mice according to our previous experiments (data not shown). Initially, we killed mice at 3 days after infection, and measured the bacterial loads as the numbers of CFU in the lung, spleen, and liver. One- to two-log decreases in the bacterial loads in the lung, spleen, and liver were found in LPS-LLO DC–immunized mice compared with LLO DC–, LPS-control DC–, and control DC-immunized mice (Figure 6). In contrast, no significant differences were found in the bacterial loads in any of the examined organs among LLO DC–, LPS-control DC–, and control DC–immunized mice. Subsequently, our survival analysis revealed that, although virtually all the mice immunized with LLO DC, LPS-control DC, and control DC died within 7 days after infection, 80% of mice immunized with LPS-LLO DC survived (Figure 7A). The differences in the survival curves were statistically significant between LPS-LLO DC–immunized mice and LLO DC–, LPS-control DC–, and control DC–immunized mice ($P < 0.0001$). Representative histology of lung tissues from each group at 3 days after infection are presented in Figure 7B. A marked decrease in lung inflammation was noted in LPS-LLO DC–immunized mice compared with LLO DC–, LPS-control DC–, and control DC–immunized mice. These results indicate that intratracheal immunization with LPS-LLO DC induced potent protective immunity against lethal respiratory infection with *L. monocytogenes*, accompanied by decreases in the bacterial load in the whole body and improved survival.

DISCUSSION

In the present study, we attempted to develop a mucosal DC vaccine for generating CTL against respiratory infections with intracellular pathogens. We showed that intratracheally administered LPS-treated BM-DC pulsed with a single immunodominant CTL epitope of *L. monocytogenes* could possibly migrate to MLN, and efficiently generate epitope-specific CTL locally as well as systemically. The generated CTL had a high capacity for IFN-γ production and potent cytotoxic activity. Furthermore, this DC immunization provided strong protection against lethal respiratory infection with *L. monocytogenes*. These data suggest that mucosal vaccination with immunodominant CTL epitope-loaded DC is an effective vaccine strategy for generating protective CTL against respiratory infections with intracellular pathogens.

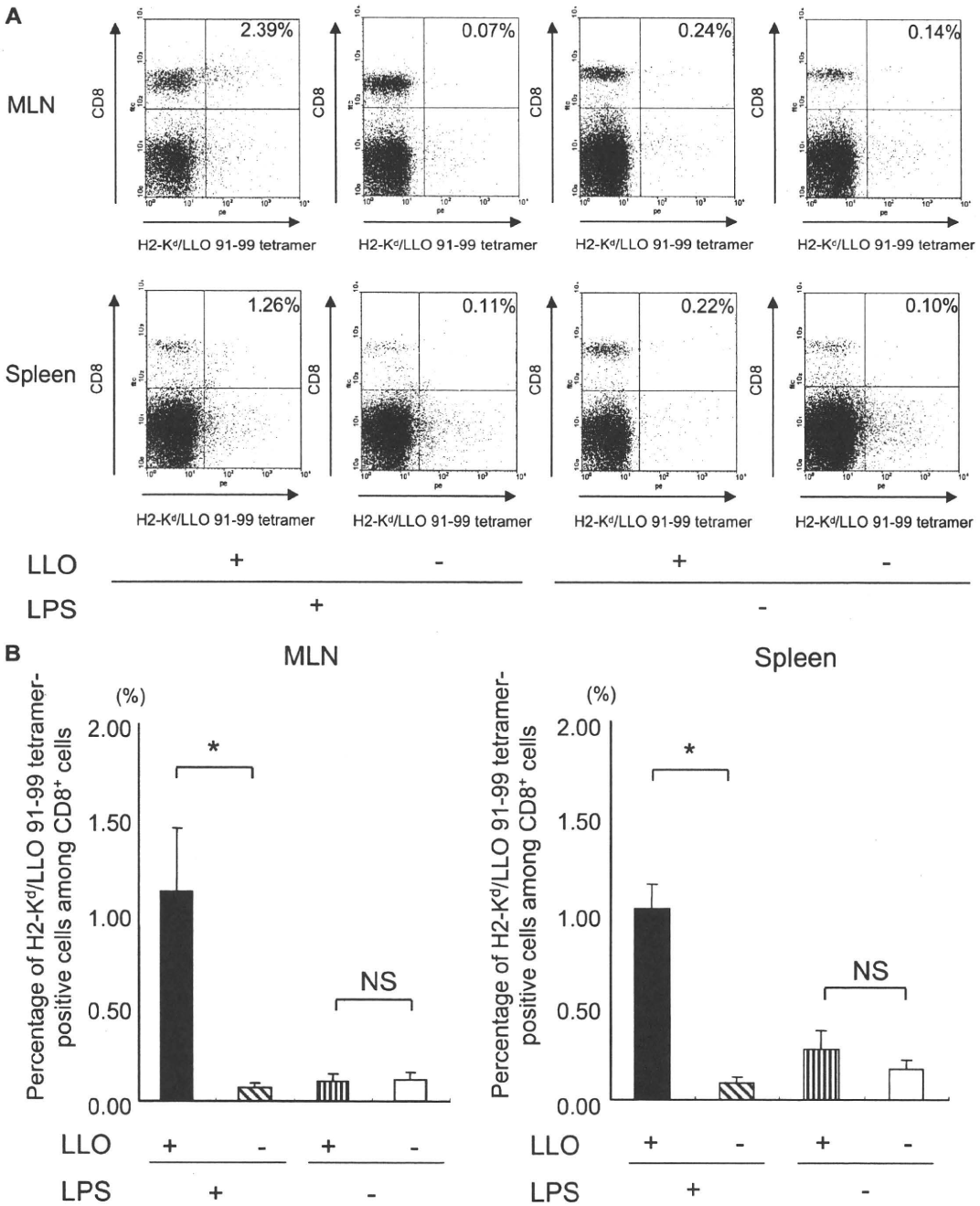

Figure 3. LLO 91-99–specific CD8$^+$ T cells in mediastinal lymph nodes (MLN) and spleens of immunized mice. Cells were harvested from MLN and spleens of mice immunized with LPS-treated LLO-pulsed DC (LPS-LLO DC), LLO-pulsed DC (LLO DC), LPS-treated DC (LPS-control DC), or control DC. LLO 91-99–specific CD8$^+$ T cells were evaluated by flow cytometry with a tetrameric LLO 91-99 H2-K^d/LLO 91-99 peptide complex. (*A*) Representative profiles of the flow cytometry analyses. (*B*) Percentages of LLO 91-99–specific CD8$^+$ T cells among the total CD8$^+$ T cells. Values are expressed as the mean ± SEM of six mice per group. *$P < 0.05$.

Unlike central lymphoid organs, T cell responses at mucosal surfaces have been shown to have Th2 polarity, depending on their inherent properties (20, 32). In the lung, intranasal delivery of a Th1-inducing antigen was shown to promote Th2-dominated responses, rather than the expected Th1 responses, suggesting that the lung microenvironment intrinsically favors the generation of Th2 responses (19). In accordance with this, several studies have revealed that intratracheal injection of BM-DC modified with particulate antigens can provoke antigen-specific Th2 immune responses in the lung. Initially, Lambrecht and coworkers (22) demonstrated that mice immunized intratracheally with ovalbumin (OVA)-pulsed BM-DC exhibited Th2 cell accumulation in the airway, eosinophilic airway inflammation, and goblet cell hyperplasia after challenge with aerosolized OVA. Other studies confirmed these findings, and DC introduced through the intratracheal route are currently used as an adjuvant to induce

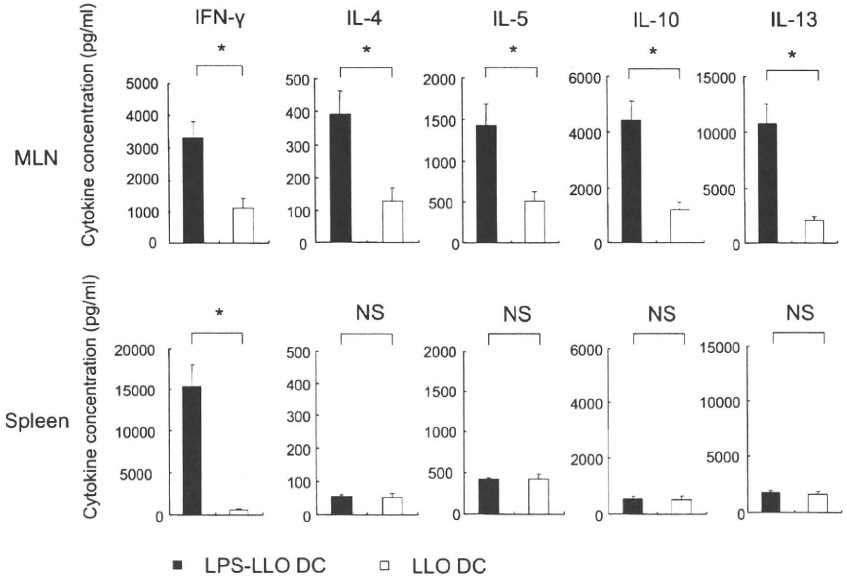

Figure 4. Cytokine production in MLN and spleens of immunized mice. Cells were harvested from MLN and spleens of mice immunized with LPS-treated LLO-pulsed DC (LPS-LLO DC, *solid bars*) or LLO-pulsed DC (LLO DC, *open bars*). The cells were cultured in the presence of LLO 91-99 peptide for 3 days and the levels of IFN-γ, IL-4, IL-5, IL-10, and IL-13 in the supernatants were measured using a cytometric bead array. Values are expressed as the mean ± SEM of six mice per group. $*P < 0.05$.

Th2 immune responses (33, 34). In the present study, however, we attempted to generate CTL responses in the lung using intratracheal injection of BM-DC. First, we intratracheally immunized mice with LLO 91-99–loaded BM-DC that had not been treated with LPS (LLO DC), but failed to induce epitope-specific CTL. Notably, after pretreatment of BM-DC with LPS, we found that intratracheal immunization with LPS-treated LLO 91-99–loaded BM-DC (LPS-LLO DC) could efficiently generate functional epitope-specific CTL. Using the tetrameric H2-K^d/LLO 91-99 peptide complex, we found that intratracheal injection of LPS-LLO DC significantly increased LLO 91-99–specific $CD8^+$ T cells in MLN, which secreted large amounts of IFN-γ in response to LLO 91-99 peptide with potent epitope-specific CTL activity. Furthermore, this vaccination protected mice against lethal respiratory infection with *L. monocytogenes*. These findings are in sharp contrast to the generation of Th2 immune responses by intratracheal DC injection, in which LPS treatment is not necessary. Together, our data indicate that intratracheal vaccination with LPS-treated DC can successfully induce functional CTL, and that, unlike the induction of Th2 immune responses, LPS treatment is essential for generating these CTL.

The detailed mechanism underlying the requirement for LPS treatment to generate functional CTL is unclear, but this effect may be accounted for by several points. First, an increase in DC migration to MLN after LPS treatment may be partly responsible for this effect. In our BM-DC, LPS treatment dramatically up-regulated mRNA expression of CCR7, a crucial chemokine receptor for mobilizing DC to draining lymph nodes, resulting in marked enhancement of DC migration to MLN. Consistent with our observations, Kuipers and colleagues (24) recently reported that LPS-stimulated BM-DC migrated more frequently to MLN after intratracheal injection than unstimulated BM-DC. Thus a relatively larger number of migrating epitope-loaded DC in MLN may be required for efficient induction of epitope-specific CTL. Second, DC maturation induced by LPS treatment may be critical. It is well known that pathogen-associated molecules, such as LPS and CpG motifs, stimulate DC to undergo phenotypic maturation with enhanced expression of immunostimulatory molecules, including MHC antigens and costimulatory molecules. In the present study, the expressions of MHC class II antigens CD80 and CD86 were enhanced in LPS-treated BM-DC (data not shown). These mature DC possess more potent antigen-presenting capacity than immature DC, leading to efficient generation of CTL. Third, cytokine production by DC in response to LPS may be necessary. LPS has been shown to stimulate DC production of Th1-skewing cytokines, such as IL-12, which are possibly involved in CTL generation (35). With

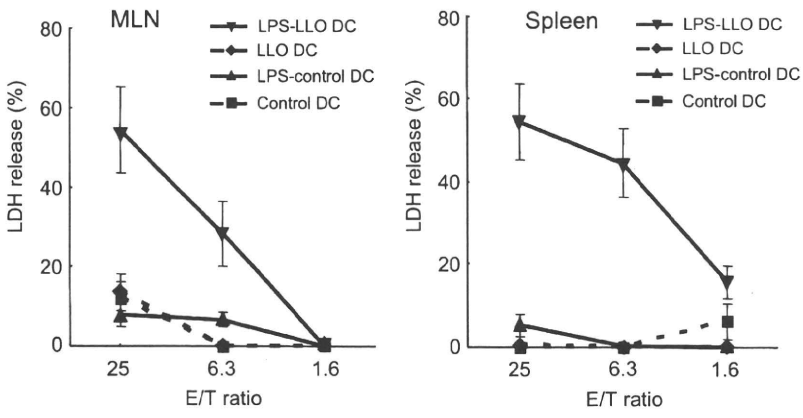

Figure 5. CTL activities in MLN and spleens of immunized mice. Cells were harvested from MLN and spleens of mice immunized with LPS-treated LLO-pulsed DC (LPS-LLO DC, *inverted triangles*), LLO-pulsed DC (LLO DC, *diamonds*), LPS-treated DC (LPS-control DC, *triangles*) or control DC (*squares*). After *in vitro* stimulation, the cells were incubated with target cells (J774 cells pulsed with LLO 91-99 peptide). The effector-to-target cell (E/T) ratios are indicated on the *x*-axis. The percentages of specific lysis of the target cells were measured using an LDH release assay. Values are expressed as the mean ± SEM of six mice per group.

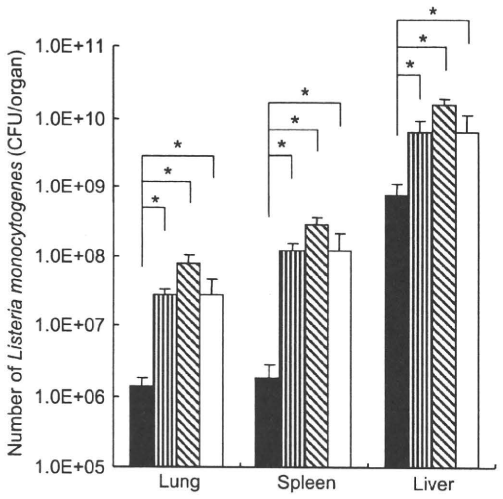

Figure 6. Protection of immunized mice against intratracheally inoculated *Listeria monocytogenes*. Mice immunized with LPS-treated LLO-pulsed DC (LPS-LLO DC, *solid bars*), LLO-pulsed DC (LLO DC, *vertically striped bars*), LPS-treated DC (LPS-control DC, *diagonally striped bars*) or control DC (*open bars*) were inoculated intratracheally with 2.5×10^4 CFU *L. monocytogenes*. The mice were killed at 3 days after the inoculation, and the numbers of bacteria in their lungs, spleens, and livers were determined by plating 10-fold dilutions of tissue homogenates on trypticase soy agar plates. Values are expressed as the mean ± SEM of seven to eight mice per group. $*P < 0.05$.

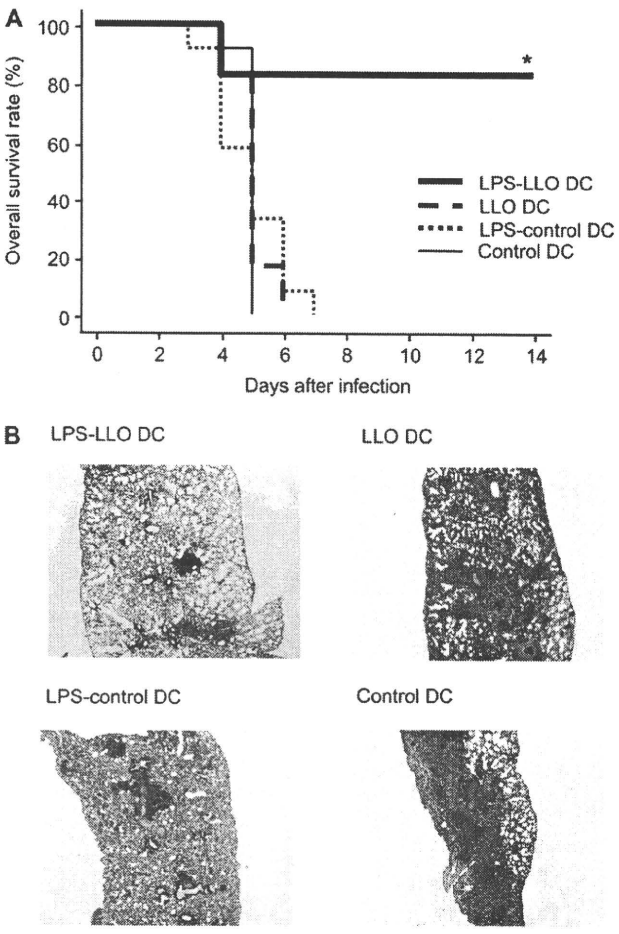

Figure 7. Protection of immunized mice against lethal respiratory infection with *L. monocytogenes*. Mice immunized with LPS-treated LLO-pulsed DC (LPS-LLO DC), LLO-pulsed DC (LLO DC), LPS-treated DC (LPS-control DC), or control DC were infected intratracheally with 2.5×10^4 CFU *L. monocytogenes*, which was equal to 5-fold the dose required to kill 50% of mice according to our previous experiments (data not shown). (*A*) Survival was recorded as the percentage of surviving animals ($n = 12$ mice per group). $*P < 0.05$, compared with mice immunized with LLO DC, LPS-control DC, or control DC. (*B*) Representative lung sections of mice immunized with LPS-LLO DC, LLO DC, LPS-control DC, and control DC at 3 days after infection with 2.5×10^4 CFU *L. monocytogenes*. Hematoxylin and eosin staining; *original magnification*: × 6.7.

respect to IL-12, however, Kuipers and coworkers (24) recently showed that intratracheal injection of LPS-stimulated OVA-pulsed BM-DC shifted OVA-specific immune responses from the Th2 phenotype to the Th1 phenotype in the lung, and this effect was independent of IL-12. In the present study, we did not examine whether particular cytokines were involved in CTL generation, and further studies will clarify this aspect.

Mucosal immune responses are most efficiently induced by administration of vaccines to mucosal sites. Thus mucosal vaccines are considered to be the ideal vaccines for protection against pathogens entering the body from mucosal surfaces (1). In addition, mucosal vaccination has been shown to effectively induce protective immunity in the whole body as well as at mucosal sites (7). In agreement with this, the present study showed that intratracheal vaccination with LPS-LLO DC generated LLO 91-99–specific $CD8^+$ T cells with high epitope-specific CTL activities in both MLN and the spleen. These results suggest that our mucosal DC vaccine can efficiently generate functional epitope-specific CTL locally as well as systemically. Interestingly, in terms of the profiles of cytokine production, vaccination with LPS-LLO DC also resulted in significant increases in the production of Th2 cytokines (IL-4, IL-5, IL-10, and IL-13) in MLN, but not in the spleen. Although the precise mechanism underlying the differences in the cytokine profiles between MLN and the spleen has not yet been determined, the distinct microenvironment and/or cytokine milieu in each organ may be responsible for these differences.

Efficient protective immunity against intracellular pathogens, including *M. tuberculosis* and *L. monocytogenes*, has been shown to require pathogen-specific CTL. CTL recognize a variety of epitopes, and among these, immunodominant CTL epitopes are defined as major epitopes that are primarily associated with the effector functions of CTL. In *M. tuberculosis*, several immunodominant CTL epitopes of protective antigens, such as antigen 85A (Ag85A), have recently been discovered. In this regard, we recently identified a new H2-D^d-restricted dominant CTL epitope of MPT51, a protective protein of *M. tuberculosis*, in BALB/c mice (36). Although pathogen-specific $CD4^+$ T cells also play a role in protection against intracellular pathogens, immunodominant epitope-specific CTL efficiently collaborate with these $CD4^+$ T cells in conferring protective immunity. Thus, our mucosal DC vaccine represents a novel strategy that boosts protective immunity against intracellular pathogens through the generation of dominant epitope-specific CTL.

In conclusion, the present study has demonstrated that a single immunodominant CTL epitope of *L. monocytogenes* can successfully confer potent protective immunity against lethal respiratory infection, together with the generation of functional epitope-specific CTL both locally and systemically, after intra-

tracheal introduction of the epitope via LPS-treated BM-DC. These results suggest that mucosal immunization with DC pulsed with immunodominant CTL epitopes is a promising strategy for effective vaccination against respiratory infections with intracellular pathogens. In addition, our data provide important knowledge that contributes toward further understanding of mucosal DC vaccines specialized for inducing functional CTL in the lung.

Conflict of Interest Statement: None of the authors has any financial relationships with commercial entities that have an interest in the subject of this manuscript.

Acknowledgments: The authors thank M. Mitsuyama (Kyoto University, Kyoto, Japan) for providing *L. monocytogenes* strain EGD and M. Okabe (Osaka University, Osaka, Japan) for providing GFP-transgenic mice. The authors also thank S. Seto and M. Uchijima (Hamamatsu University School of Medicine, Hamamatsu, Japan) for their helpful advice concerning the treatment of *L. monocytogenes*.

References

1. Kallenius G, Pawlowski A, Brandtzaeg P, Svenson S. Should a new tuberculosis vaccine be administered intranasally? *Tuberculosis (Edinb)* 2007;87:257–266.
2. Kaufmann SH. Recent findings in immunology give tuberculosis vaccines a new boost. *Trends Immunol* 2005;26:660–667.
3. Nakamura Y, Suda T, Nagata T, Aoshi T, Uchijima M, Yoshida A, Chida K, Koide Y, Nakamura H. Induction of protective immunity to *Listeria monocytogenes* with dendritic cells retrovirally transduced with a cytotoxic T lymphocyte epitope minigene. *Infect Immun* 2003; 71:1748–1754.
4. Hashimoto D, Nagata T, Uchijima M, Seto S, Suda T, Chida K, Miyoshi H, Nakamura H, Koide Y. Intratracheal administration of third-generation lentivirus vector encoding MPT51 from *Mycobacterium tuberculosis* induces specific CD8+ T-cell responses in the lung. *Vaccine* 2008;26:5095–5100.
5. Nakano H, Nagata T, Suda T, Tanaka T, Aoshi T, Uchijima M, Kuwayama S, Kanamaru N, Chida K, Nakamura H, *et al.* Immunization with dendritic cells retrovirally transduced with mycobacterial antigen 85A gene elicits the specific cellular immunity including cytotoxic T-lymphocyte activity specific to an epitope on antigen 85A. *Vaccine* 2006;24:2110–2119.
6. Enomoto N, Nagata T, Suda T, Uchijima M, Nakamura Y, Chida K, Nakamura H, Koide Y. Immunization with dendritic cells loaded with alpha-galactosylceramide at priming phase, but not at boosting phase, enhances cytotoxic T lymphocyte activity against infection by intracellular bacteria. *FEMS Immunol Med Microbiol* 2007;51:350–362.
7. Wu HY, Nikolova EB, Beagley KW, Eldridge JH, Russell MW. Development of antibody-secreting cells and antigen-specific T cells in cervical lymph nodes after intranasal immunization. *Infect Immun* 1997;65:227–235.
8. Dietrich J, Andersen C, Rappuoli R, Doherty TM, Jensen CG, Andersen P. Mucosal administration of Ag85B-ESAT-6 protects against infection with *Mycobacterium tuberculosis* and boosts prior bacillus Calmette-Guerin immunity. *J Immunol* 2006;177:6353–6360.
9. Gheorghiu M. BCG-induced mucosal immune responses. *Int J Immunopharmacol* 1994;16:435–444.
10. Xing Z, Lichty BD. Use of recombinant virus-vectored tuberculosis vaccines for respiratory mucosal immunization. *Tuberculosis (Edinb)* 2006;86:211–217.
11. Chen L, Wang J, Zganiacz A, Xing Z. Single intranasal mucosal *Mycobacterium bovis* BCG vaccination confers improved protection compared with subcutaneous vaccination against pulmonary tuberculosis. *Infect Immun* 2004;72:238–246.
12. Santosuosso M, Zhang X, McCormick S, Wang J, Hitt M, Xing Z. Mechanisms of mucosal and parenteral tuberculosis vaccinations: adenoviral-based mucosal immunization preferentially elicits sustained accumulation of immune protective CD4 and CD8 T cells within the airway lumen. *J Immunol* 2005;174:7986–7994.
13. Goonetilleke NP, McShane H, Hannan CM, Anderson RJ, Brookes RH, Hill AV. Enhanced immunogenicity and protective efficacy against *Mycobacterium tuberculosis* of bacille Calmette-Guerin vaccine using mucosal administration and boosting with a recombinant modified vaccinia virus Ankara. *J Immunol* 2003;171:1602–1609.
14. Naito T, Suda T, Suzuki K, Nakamura Y, Inui N, Sato J, Chida K, Nakamura H. Lung dendritic cells have a potent capability to induce production of immunoglobulin A. *Am J Respir Cell Mol Biol* 2008;38: 161–167.
15. Tsuchiya T, Chida K, Suda T, Schneeberger EE, Nakamura H. Dendritic cell involvement in pulmonary granuloma formation elicited by bacillus Calmette-Guerin in rats. *Am J Respir Crit Care Med* 2002; 165:1640–1646.
16. Todate A, Chida K, Suda T, Imokawa S, Sato J, Ide K, Tsuchiya T, Inui N, Nakamura Y, Asada K, *et al.* Increased numbers of dendritic cells in the bronchiolar tissues of diffuse panbronchiolitis. *Am J Respir Crit Care Med* 2000;162:148–153.
17. Suzuki K, Suda T, Naito T, Ide K, Chida K, Nakamura H. Impaired toll-like receptor 9 expression in alveolar macrophages with no sensitivity to CpG DNA. *Am J Respir Crit Care Med* 2005;171:707–713.
18. Herrick CA, MacLeod H, Glusac E, Tigelaar RE, Bottomly K. Th2 responses induced by epicutaneous or inhalational protein exposure are differentially dependent on IL-4. *J Clin Invest* 2000;105:765–775.
19. Constant SL, Lee KS, Bottomly K. Site of antigen delivery can influence T cell priming: pulmonary environment promotes preferential Th2-type differentiation. *Eur J Immunol* 2000;30:840–847.
20. Jones HP, Hodge LM, Fujihashi K, Kiyono H, McGhee JR, Simecka JW. The pulmonary environment promotes Th2 cell responses after nasal-pulmonary immunization with antigen alone, but Th1 responses are induced during instances of intense immune stimulation. *J Immunol* 2001;167:4518–4526.
21. Uchijima M, Yoshida A, Nagata T, Koide Y. Optimization of codon usage of plasmid DNA vaccine is required for the effective MHC class I-restricted T cell responses against an intracellular bacterium. *J Immunol* 1998;161:5594–5599.
22. Lambrecht BN, De Veerman M, Coyle AJ, Gutierrez-Ramos JC, Thielemans K, Pauwels RA. Myeloid dendritic cells induce Th2 responses to inhaled antigen, leading to eosinophilic airway inflammation. *J Clin Invest* 2000;106:551–559.
23. Forster R, Davalos-Misslitz AC, Rot A. CCR7 and its ligands: balancing immunity and tolerance. *Nat Rev Immunol* 2008;8:362–371.
24. Kuipers H, Hijdra D, De Vries VC, Hammad H, Prins JB, Coyle AJ, Hoogsteden HC, Lambrecht BN. Lipopolysaccharide-induced suppression of airway Th2 responses does not require IL-12 production by dendritic cells. *J Immunol* 2003;171:3645–3654.
25. Martin-Fontecha A, Sebastiani S, Hopken UE, Uguccioni M, Lipp M, Lanzavecchia A, Sallusto F. Regulation of dendritic cell migration to the draining lymph node: impact on T lymphocyte traffic and priming. *J Exp Med* 2003;198:615–621.
26. Hintzen G, Ohl L, del Rio ML, Rodriguez-Barbosa JI, Pabst O, Kocks JR, Krege J, Hardtke S, Forster R. Induction of tolerance to innocuous inhaled antigen relies on a CCR7-dependent dendritic cell-mediated antigen transport to the bronchial lymph node. *J Immunol* 2006;177: 7346–7354.
27. Ohl L, Mohaupt M, Czeloth N, Hintzen G, Kiafard Z, Zwirner J, Blankenstein T, Henning G, Forster R. CCR7 governs skin dendritic cell migration under inflammatory and steady-state conditions. *Immunity* 2004;21:279–288.
28. Dieu MC, Vanbervliet B, Vicari A, Bridon JM, Oldham E, Ait-Yahia S, Briere F, Zlotnik A, Lebecque S, Caux C. Selective recruitment of immature and mature dendritic cells by distinct chemokines expressed in different anatomic sites. *J Exp Med* 1998;188:373–386.
29. Osterholzer JJ, Ames T, Polak T, Sonstein J, Moore BB, Chensue SW, Toews GB, Curtis JL. CCR2 and CCR6, but not endothelial selectins, mediate the accumulation of immature dendritic cells within the lungs of mice in response to particulate antigen. *J Immunol* 2005;175: 874–883.
30. Stumbles PA, Strickland DH, Pimm CL, Proksch SF, Marsh AM, McWilliam AS, Bosco A, Tobagus I, Thomas JA, Napoli S, *et al.* Regulation of dendritic cell recruitment into resting and inflamed airway epithelium: use of alternative chemokine receptors as a function of inducing stimulus. *J Immunol* 2001;167:228–234.
31. Lambrecht BN, Pauwels RA, Fazekas De St Groth B. Induction of rapid T cell activation, division, and recirculation by intratracheal injection of dendritic cells in a TCR transgenic model. *J Immunol* 2000;164: 2937–2946.
32. Stumbles PA, Thomas JA, Pimm CL, Lee PT, Venaille TJ, Proksch S, Holt PG. Resting respiratory tract dendritic cells preferentially stimulate T helper cell type 2 (Th2) responses and require obligatory cytokine signals for induction of Th1 immunity. *J Exp Med* 1998;188: 2019–2031.
33. van Rijt LS, Jung S, Kleinjan A, Vos N, Willart M, Duez C, Hoogsteden HC, Lambrecht BN. In vivo depletion of lung CD11c+ dendritic cells during allergen challenge abrogates the characteristic features of asthma. *J Exp Med* 2005;201:981–991.

34. Miyahara N, Ohnishi H, Matsuda H, Miyahara S, Takeda K, Koya T, Matsubara S, Okamoto M, Dakhama A, Haribabu B, *et al.* Leukotriene B4 receptor 1 expression on dendritic cells is required for the development of Th2 responses and allergen-induced airway hyperresponsiveness. *J Immunol* 2008;181:1170–1178.
35. Medzhitov R. Toll-like receptors and innate immunity. *Nat Rev Immunol* 2001;1:135–145.
36. Suzuki M, Aoshi T, Nagata T, Koide Y. Identification of murine H2-Dd- and H2-Ab-restricted T-cell epitopes on a novel protective antigen, MPT51, of Mycobacterium tuberculosis. *Infect Immun* 2004;72:3829–3837.

European Journal of Immunology

The cellular niche of *Listeria monocytogenes* infection changes rapidly in the spleen

Taiki Aoshi[1], Javier A. Carrero[1], Vjollca Konjufca[1], Yukio Koide[2], Emil R. Unanue[1] and Mark J. Miller[1]

[1] Department of Pathology and Immunology, Washington University School of Medicine, St. Louis, MO, USA
[2] Department of Infectious Diseases, Hamamatsu University School of Medicine, Hamamatsu, Shizuoka, Japan

The spleen is an important organ for the host response to systemic bacterial infections. Many cell types and cell surface receptors have been shown to play role in the capture and control of bacteria, yet these are often studied individually and a coherent picture has yet to emerge of how various phagocytes collaborate to control bacterial infection. We analyzed the cellular distribution of *Listeria monocytogenes* (LM) *in situ* during the early phase of infection. Using an immunohistochemistry approach, five distinct phagocyte populations contained LM after i.v. challenge and accounted for roughly all bacterial signal in tissue sections. Our analysis showed that LM was initially captured by a wide range of phagocytes in the marginal zone, where the growth of LM appeared to be controlled. The cellular distribution of LM within phagocyte populations changed rapidly during the first few hours, decreasing in marginal zone macrophages and transiently increasing in CD11c$^+$ DC. After 4–6 h LM was transported to the periarteriolar lymphoid sheath where the infective foci developed and LM grew exponentially.

Key words: Bacterial infection · DC · *Listeria monocytogenes* · Macrophages · Spleen

Supporting Information available online

Introduction

The spleen is an important site for host responses to bacterial infection [1, 2]. Within the spleen, bacteria may encounter various tissue resident phagocytes including macrophages, DC, and neutrophils [3, 4]. Marginal zone macrophages (MZM) are positioned along the outer layer of the marginal sinus where they have direct access to bacteria entering the spleen from the circulation. These macrophages express MARCO (macrophage receptor with collagenous structure), a type-1 scavenger receptor, related to the SR-A family of receptors [5], which recognizes bacterial cell-wall-associated polyanions [6]. MZM also express the C-type lectin, SIGN-R1. SIGN-R1 binds dextran [7] and facilitates the capture of polysaccharide antigens on bacteria such as *Streptococcus pneumoniae* [8]. A separate class of MZM, the metallophilic MZM (MMM), localize between the inner marginal sinus and the B-cell follicle [9]. These cells recognize sialic acid and LPS from *Neiseria meningitidis* [10] through Siglec-1 (sialic-acid-binding-Ig-like-lectin 1) [11, 12]. MMM have also been shown to produce interferon during Herpes simplex virus infection [13], but their role in bacterial infection is unclear, although it was reported that they produce CCL2 [14].

Neutrophils play a crucial role in controlling bacterial infection [15–19]. They are present in the marginal zone (MZ) and

Correspondence: Dr. Mark J. Miller
e-mail: miller@pathology.wustl.edu

red pulp (RP) of the spleen and therefore have access to circulating bacteria and bacteria released from infected splenocytes. Also within the MZ of the spleen resides a population of DC recognized with the antibody 33D1 [20], which have been shown to efficiently present antigens to $CD4^+$ T cells [21]. The location of these cells in the MZ suggests that they may participate in the capture of bacteria in the circulation. Macrophages are also present in the RP [22]. These macrophages are $F4/80^+$ and primarily serve to remove dying red blood cells and other debris from the circulation [23].

We used intravenous LM infection [24] and a semi-quantitative immunofluorescence approach to investigate the capture and clearance of bacteria in the spleen. Previous histological studies showed that LM was trapped in the MZ of the spleen [25–27]. Clodronate-liposome depletion of MZ macrophages *in vivo* indicated that they were required for initial LM capture and control, but were dispensable for specific T-cell-mediated immunity [25]. At 24 h following infection, LM was found primarily within $CD11b^+$ and, to a less extent, $CD11c^+$ cells [27]. More recently, $CD8\alpha^+$ DC were found to be the primary cell type containing viable bacteria early after infection (1–3 h) [28]. Other studies have detected LM exclusively in SIGN-$R1^+$ MZM and not $CD11c^+$ DC very early after infection [14]. Here, we identified five phagocyte populations that contained the bulk of LM after i.v. challenge. During the time when LM was in the MZ, its colocalization with MZM decreased dramatically. This shift in the cellular niche of LM *in vivo* has important implications for bacterial pathogenesis and protective host responses in the spleen.

Results

LM enters a wide variety of phagocytes immediately after challenge

We found that the recovery of LM (EGD)-infected host cells from spleen was unreliable; ~90% of LM CFU were lost in the process of isolating phagocytes and making single cell suspensions (Supporting Information Fig. 1). As an alternative, we developed an antibody staining approach, by which we identified five distinct phagocyte populations in spleen cryosections (Fig. 1 and Supporting Information Fig. 2). We observed three distinct macrophage subsets in their expected locations: $F4/80^+$ in the RP, $MARCO^+$ MZM in the outer MZ, and MOMA-1^+ MMM in the inner MZ (Fig. 1A–C) [5, 9, 22, 29]. Nearly all ER-$TR9^+$ MZM co-stained with antibodies to MARCO, suggesting that SIGN-$R1^+$ cells are actually a subset of $MARCO^+$ MZM (Fig. 1D). The $CD11b^{hi}$ cells in our images appeared to be neutrophils, since they were smaller and rounder than macrophages and localized outside the white pulp (Fig. 1B, C, and F). Moreover, >95% of $CD11b^+$ cells were Gr-1^+ (Ly6G) and $F4/80^-$ in co-stained sections (Fig. 1E and F). However, Gr-1 also reacts with the epitope Ly6C expressed on a number of other cell types, including inflammatory macrophages, making it difficult to define the $CD11b^+$ population unambiguously. We found $CD11c^+$ cells

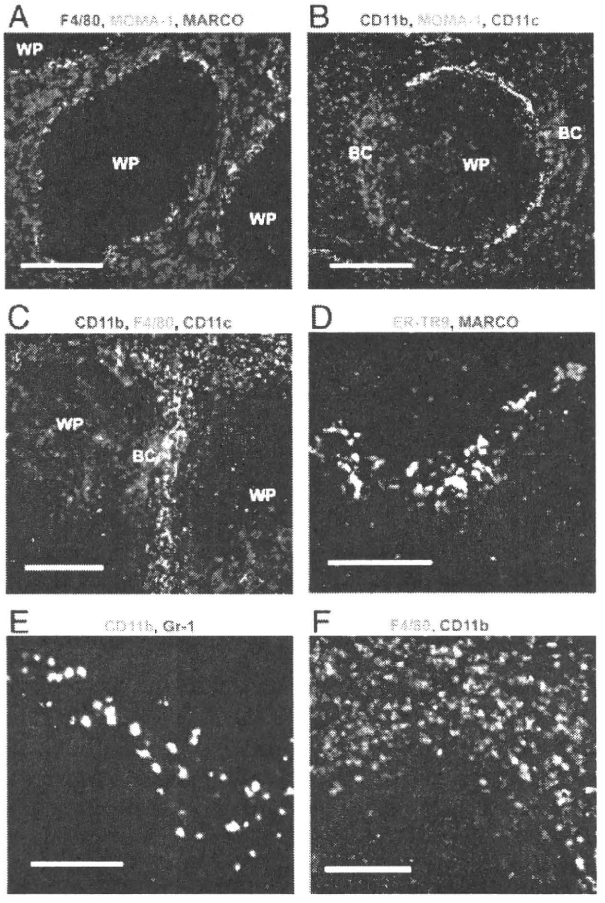

Figure 1. Histological characterization of resident phagocytes in the spleen. Cryosections from normal BALB/c mice were stained with different combinations of host cell markers to demonstrate staining specificity. (A) Anti-F4/80 (blue), anti-MOMA-1 (green), and anti-MARCO (red). (B) Anti-CD11b (blue), MOMA-1 (green), and CD11c (red). (C) Anti-CD11b (blue), anti-F4/80 (green), and anti-CD11c (red). (D) Anti-ER-TR9 (green) and anti-MARCO (red). Nearly all ER-$TR9^+$ cells also express MARCO (yellow), suggesting that they are a subset of the $MARCO^+$ MZM. (E) Anti-Gr-1 (green) and anti-CD11b (red). Approximately, 95% of $CD11b^+$ cells are small, round and co-stained with Gr-1. (F) $CD11b^+$ cells do not stain with F4/80, anti-F4/80 (green) and anti-CD11b (red). Scale bar = 200 μm in (A–C) and 100 μm in (D–F). Images are representative of three independent experiments. WP: white pulp. BC: bridging channel.

localized to the periarteriolar lymphoid sheath (PALS), the bridging channel and distributed sparsely in the RP and the MZ (Fig. 1B and C), also consistent with previous reports [30–32].

To reveal the host cells that interacted with LM immediately after infection, mice were injected with LM and sacrificed from minutes to hours later. Cryosections were prepared, stained with antibodies to LM and various host cell markers and the percentage of LM fluorescence signal overlap with each phagocyte surface marker (*i.e.* colocalization coefficient) was determined as described previously [33] (Fig. 2).

In contrast to previous reports [14, 28], LM entered a wide range of host phagocytes in the spleen (Fig. 2A). The percentage

of LM signal colocalized with each host cell type was as follows: F4/80$^+$ macrophages (26%), MARCO$^+$ macrophages (30%), MOMA-1$^+$ macrophages (19%), CD11b$^+$ cells (18%), and CD11c$^+$ DC (18%) and B220$^+$ cells (10%) (Fig. 2B). We included B220 staining as an internal negative control, because lymphocytes including B cells are not directly infected by LM. LM colocalization with B220 ranged from 5 to 10% in individual experiments. However, the covariance of LM and B220 signal was consistently negative (Pearson's correlation coefficient = −0.25), indicating that colocalization was less than that expected by chance alone, thus making B220 a suitable negative control. (The B220 stain may include plasmacytoid DC (pDC), but their contribution should be negligible since they represent less than 1% of spleen cells while B cells represent close to 50%.)

Histological analyses were performed at different concentrations of LM including those over the LD_{50} dose (Fig. 2C). At the 10^6 dose, most phagocytes contained a single bacterium (Fig. 2A). At a higher dose (10^8), increased variation was observed with many cells containing one LM and others containing small clusters of LM (Fig. 2C). Despite a 100-fold increase in dose (from 10^6 to 10^8), the cellular distribution of LM remained remarkably similar at 30 min after injection (compare panel 2D with 2B in Fig. 2), with the exception that more LM was found in CD11b$^+$ cells with the larger inocula (38% up from 18%). We also gave mice a 20-fold lower dose of LM (5×10^4) and examined its distribution. Although the number of bacteria in each section was small and highly variable, we found numerous examples of LM colocalized to each of the five phagocyte populations (Supporting Information Fig. 3A and B), similar to experiments using 10^6 LM.

We also examined the colocalization of bacteria in a sublethal infection using attenuated LM strain MORO-2 ($LD_{50} \sim 3 \times 10^6$) [34], which behaves normally during the first few hours of infection, but can replicate only approximately three times in the host cytosoplasm due to a deficiency in lipoic acid utilization. The cellular distribution of 10^6 MORO-2 was indistinguishable from experiments using 10^6 EGD (Supporting Information Fig. 3C and D).

Next, we compared LM uptake with other known substrates of phagocytosis: fluorescent polystyrene beads and FITC-conjugated dextrans. At 30 min after injection, fluorescent beads were taken up by MZM and, to a much lesser extent, by CD11c$^+$ DC (Fig. 2E). The majority of beads (~76%) were associated with MARCO$^+$ cells, ~40% with MOMA-1$^+$ MMM, and <20% with CD11c$^+$ DC. Few, if any, beads were associated with CD11b$^+$ and F4/80$^+$ cells. FITC-conjugated dextran, which has been shown to be taken up specifically by MZM (MARCO$^+$ ER-TR9$^+$) *via* SIGN-R1 [7], was captured efficiently by MARCO$^+$ cells and accumulated to high levels by 30 min (Fig. 2F). The other phagocyte populations examined showed only background levels of colocalization with dextran (Fig. 2F), validating our analysis. Thus, the trapping of LM was unexpectedly promiscuous compared with the uptake of fluorescent beads and dextran.

It is important to note that the initial trapping compartment of LM was capable of controlling infection. We have infected wild-type 129/SvEv, as well as type I and type II interferon-deficient mice (IFNAR and IFNGR) and found limited to no growth of bacteria between 30 min and 4 h post-infection in the spleen (Fig. 2G). This would suggest that the net ability of the MZ cells is to control LM independent of tonic interferon signaling.

The cellular niche of LM changes rapidly

The fate of LM in phagocytes was examined during the first hours of infection. From 30 min to 6 h, the amount of LM *per* cell in F4/80$^+$ and CD11c$^+$ cells held steady without an appreciable increase (Fig. 3A). For MOMA-1$^+$ cells, a slight increase at 2 h was observed; however, there was no significant difference between 30 min and 6 h. In contrast, LM signal in MARCO$^+$ and CD11b$^+$ cells decreased significantly (Fig. 3A). To determine whether this result also held true for ER-TR9$^+$ MZM, we examined LM colocalization with ER-TR9 (bright yellow spots in Fig. 3B) and found it decreased significantly at 2 and 6 h (Fig. 3B and C). In addition, we observed a marked decrease in covariance between LM and ER-TR9 signals over the first 6 h after infection (Fig. 3D). The total LM pixel *per* image remained relatively stable over this time (Fig. 3E) and was well correlated to the actual CFU counts *per* spleen (Fig. 3F). Moreover, host cell signal remained constant, with the exception of CD11b, which increased roughly 50% between 30 min and 6 h (Fig. 3G). We believe that the increased in CD11b$^+$ signal most likely represents the infiltration of cells because the signal increases rapidly and we did not detect a gradual rise in signal intensity on a *per* cell basis between 0.5 and 6 h (data not shown). After 6 h, LM is also detected in the PALS, the site of rapid exponential growth of LM in the spleen [27, 35].

At 12 h, approximately 40% of the LM signal in the MZ was found in CD11c$^+$ cells (Fig. 4A), while about 20% was found in each of the F4/80$^+$, MOMA-1$^+$, and CD11b$^+$ populations, similar to the 30 min time point. In contrast, only 5% of the LM signal was found in MARCO$^+$ MZM (compared with 30% at 30 min). By 24 h, when LM infection was confined primarily to the PALS, the cellular distribution of LM changed further (Fig. 4B). The majority of infected cells at 24 h were CD11b$^+$ cells (54%) and LM was barely detectable in MARCO$^+$ MZM (~2% colocalization). The percentage of colocalization with CD11c$^+$ cells also fell sharply to 22%. Both, F4/80$^+$ macrophages and MOMA-1$^+$ cells continued to show evidence of LM infection with colocalization coefficients of 17 and 18%, respectively.

Discussion

Defining the cellular niche occupied by bacteria in the spleen is fundamental for understanding how bacterial pathogenesis proceeds *in vivo* and how the host mounts a protective immune response. Our analysis showed that LM was taken up initially by a broad range of phagocytic cells, including macrophages (MARCO$^+$, ERT-R9$^+$, and F4/80), granulocytes (CD11b$^+$, Gr-1$^+$ cells) and DC (CD11c$^+$), in general agreement with a previous histological study [26]. These results contrast sharply with the conclusions of others that LM was captured exclusively by CD8a$^+$ DC [28] or

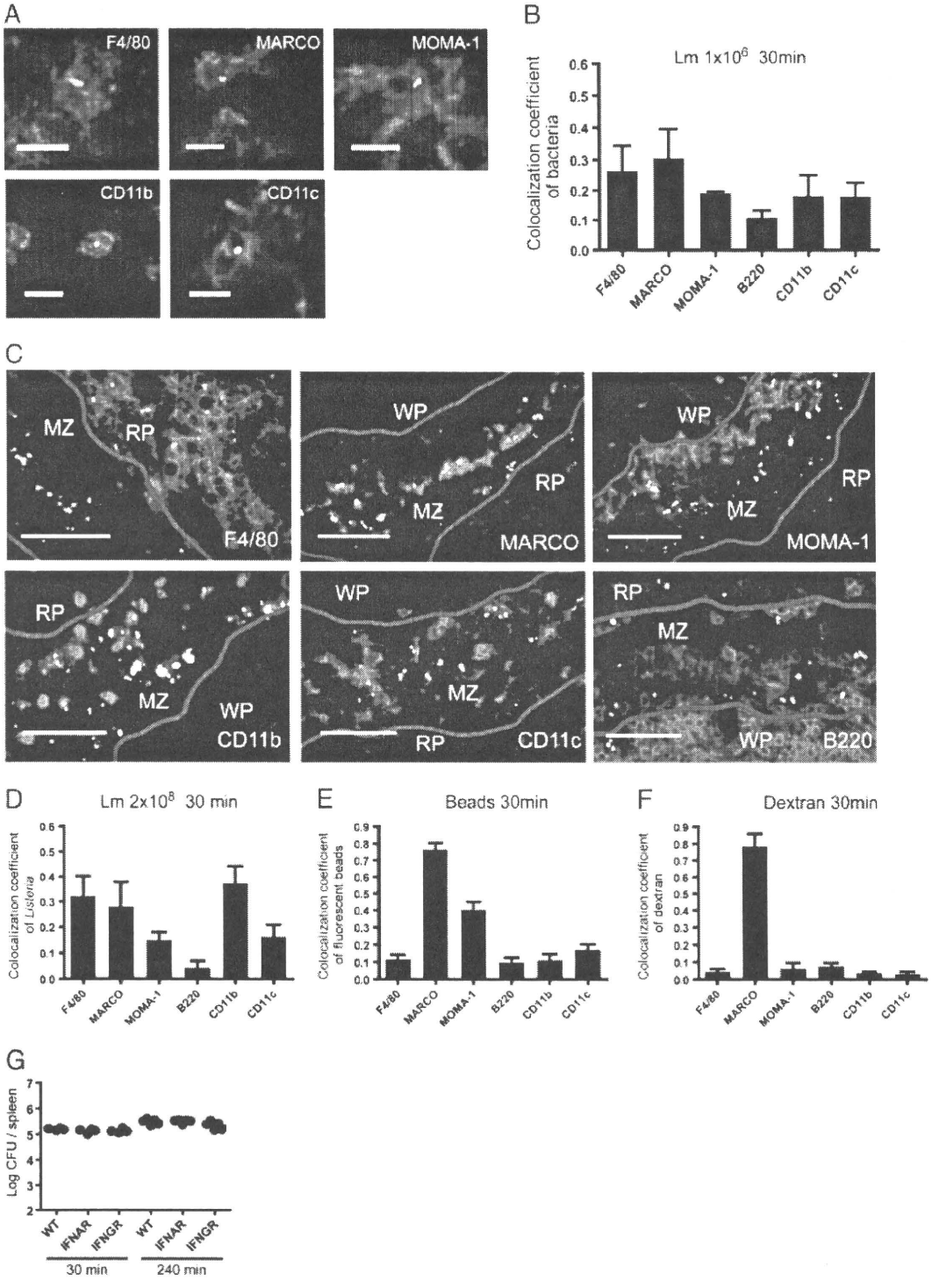

Figure 2. LM is broadly distributed in splenocytes immediately after i.v. infection. (A) Infected host cells in stained cryosections 30 min following infection with 10^6 EGD strain of LM. LM (green) and host cell markers (red). Scale bar = 10 μm. Images are representative of three independent experiments. (B) LM colocalization with host cell types. Bars represent mean+SD of at least 30 images *per* each cell type. (C) Spleens at 30 min post infection with 2×10^8 LM. Cryosections were stained with phalloidin-Alexa Fluor 350, anti-LM (green) and indicated host cell markers (red). Yellow represents colocalization between LM and stained host-cells. Blue lines represent the edge of the MZ determined by phalloidin staining. Scale bar = 50 μm. (D) Colocalization analysis of (D) 2×10^8 LM, (E) 7.2×10^8 fluorescent 1.0 μm beads, and (F) 200 μg of 70 kDa FITC-conjugated dextran with splenic phagocytes 30 min after i.v. injection. Bars represent mean+SD of ten images *per* cell type. (G) 129/SvEv, IFNAR, and IFNGR mice were infected intravenously with 10^7 CFU of LM EGD strain and spleen colony counts were determined at 30 and 240 min post infection. MZ: marginal zone; RP: red pulp; WP: white pulp.

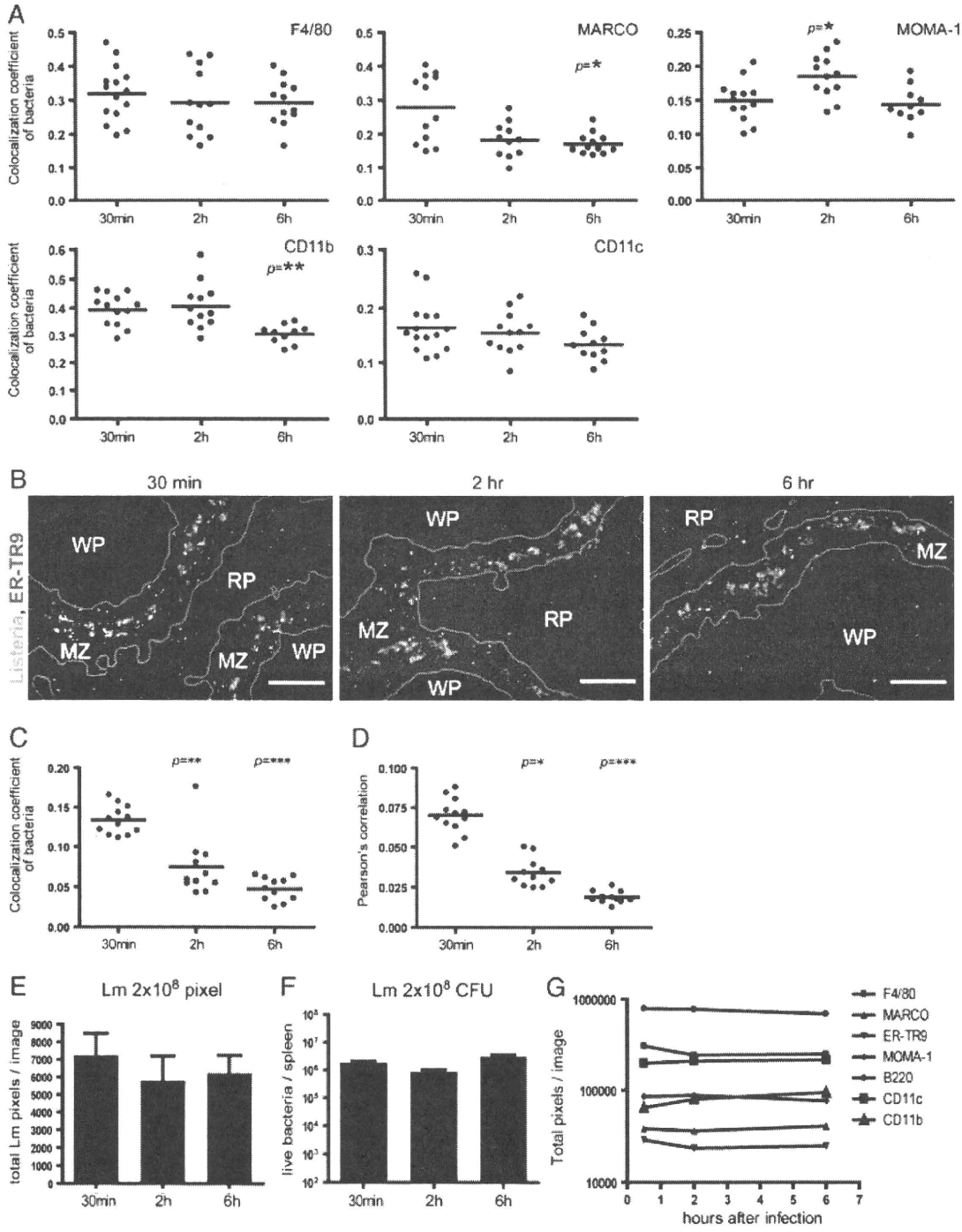

Figure 3. LM signal decreases in MZM 0.5–6 h post-infection. (A) The colocalization coefficients of LM and host cell markers over time. Scatter plots show mean values for individual images and pooled means. (B) Spleen sections from mice infected with 2×10^8 LM at 30 min, 2 h, and 6 h. Cryosections were stained with phallodin-Alexa Fluor 350, anti-LM (green) and anti-SIGNR1 (red). Colocalization between LM and host-cells appears yellow in the image. Blue lines highlight the MZ edge drawn based on phalloidin staining. Scale bar = 100 μm. Images are representative of ten images *per* time point. (C) Colocalization of LM in ER-TR9$^+$ cells and (D) covariance of LM and ER-TR9 signal (Pearson's correlation), at increasing times after infection. Each dot is the mean value of a single image and pooled means are shown. (E) LM signal in pixels *per* image at 30 min, 2 h, and 6 h post infection (2×10^8 LM). Bars show mean+SD of 50 images *per* time point. (F) CFU *per* spleen 30 min, 2 h, and 6 h post infection (2×10^8 LM). Bars show mean+SD, five mice *per* group. (G) Host cell signal expressed in pixels *per* image at increasing times after infection. Graph shows mean of 12 images *per* group. All data are representative of three independent experiments with similar results. MZ: marginal zone; RP: red pulp; WP: white pulp.

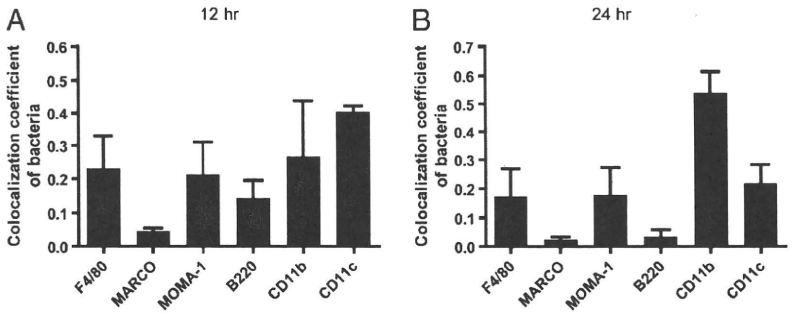

Figure 4. Host cell distribution of LM 12 and 24 h post infection. LM colocalization with splenic phagocytes 12 h (A) and 24 h (B) after infection. Bars represent mean+SD of ten images *per* cell type. Bar graphs are representative of three independent experiments. LM disappears rapidly from MARCO$^+$ MZM, but increases transiently in CD11c$^+$ cells.

ER-TR9$^+$ macrophages [14]. Histological studies from independent groups concur that LM associates with resident macrophages in the MZ for several hours after infection, although the characterization of macrophages differed depending on the markers used to detect them [14, 25–27]. Neuenhahn *et al.* [28] detected only viable LM present in splenocytes isolated by cell sorting, but because MZM are difficult to recover from spleen tissue, these cells could be easily missed during data analysis.

We used a panel of five different antibodies to provide a comprehensive histological view of early LM infection in the spleen. The criteria for including antibodies in our analysis were (i) staining must be highly reproducible and the results entirely consistent with classical histological studies with regard to the morphology and anatomical location of splenic DC, MZM, metallophilic macrophages, granulocytes, and lymphocytes [4, 9, 31, 32, 36, 37], (ii) antibodies must stain distinct splenocyte populations with minimal overlap (verified by co-staining), and (iii) the percent colocalization with LM and each host cell marker must be reproducible and the colocalized LM signal must add up to ~ 100% of the total LM signal in our sections (*i.e.* to ensure that no major splenocyte populations are missed). Our analysis focused on the early stages of LM infection but it will be important to examine other splenocyte populations such as inflammatory monocytes, pDC, and tumor necrosis factor alpha and inducible nitric oxide synthase producing DC (Tip DC) [38, 39] at later times.

In addition, we assessed the robustness of our colocalization analysis with several control experiments. We found dextran colocalized strongly with MZM (MARCO$^+$), but not other phagocytes, consistent with the fact that MZM express the dextran receptor SIGN-R1 [5]. Fluorescent beads were taken up by MARCO$^+$ and MOMA-1$^+$ macrophages, to a much lesser extent by CD11c$^+$ cells and were undetectable in CD11b$^+$ cells. The initial cellular niche of LM was strikingly promiscuous and our data suggest that LM might enter host cells *via* multiple receptors and phagocytic pathways.

During the first 4–6 h, when bacteria are located primarily in the MZ, LM growth appeared to be controlled. It was not only until LM was transported to the PALS that the exponential phase of LM growth took place. During this period the host cell distribution changed: the number of LM in MARCO$^+$ (and ER-TR9$^+$) macrophages decreased during the first few hours of infection, while it persisted in other cell types, such as CD11c$^+$ DC and MOMA-1$^+$ MMM. Whether the apparent control reflects a cytocidal activity of the MZM or is a reflection of cellular dynamics and turnover is not clear at this time. However, the capture of LM by MZM is undoubtedly important since clodronate-liposome depletion of these phagocytes augmented infection. Experiments are in progress to elucidate the mechanisms of LM control in the MZ, but our initial studies (Fig. 2G) indicate that this control is independent of either interferon-gamma or type-1 interferons. To note is that MARCO- and SIGN-R1-deficient mice were highly susceptible to pneumococcal infection [8, 40]. It will be interesting to compare and contrast LM infection with other bacteria such as *Staphylococcus* and *Salmonella* to determine whether the MZ control extends across bacterial species and possibly to viruses, as seen in LCMV infection [41, 42]. It is noteworthy that although RP macrophages do not appear to be listericidal, they apparently fail to support the proliferation of LM, since we did not detect an increase in the amount of LM in the F4/80$^+$ cells during the timeframe of our experiments.

In contrast to the MZ stage of infection, LM signal increased explosively in the PALS from 12-24 h. The preferential replication of LM in the PALS might reflect decreased bactericidal capacity or alternatively PALS resident cells, such as DC, might be more permissive for LM proliferation. In fact, we observed a significant increase of LM in DC over the first 12 h of infection. Moreover the heightened and very extensive lymphocyte apoptosis in PALS has been shown to be in great part responsible for such strong expansion of LM [43].

Materials and methods

Mice

BALB/cJ mice were obtained from the Jackson Laboratory (Bar Harbor, ME) and were maintained and bred under specific pathogen free conditions in the Washington University mouse facility, in accordance with the guidelines of the Washington

University Committee for the Humane Care of Laboratory Animals and with National Institutes of Health guidelines on laboratory animal welfare.

Bacteria and fluorescent reagents

LM strain EGD was stored as frozen glycerol stocks ($\sim 1 \times 10^9$/mL) at −80°C. LM numbers in the spleen were estimated by determining CFU from tissue homogenates using standard procedures. For early time point experiments (30 min–6 h), bacteria were cultured in BHI medium and harvested during log phase growth for inoculation. LM concentrations in liquid cultures were estimated by optical density measurements using standard growth curves. For 12 and 24 time points, frozen stocks were thawed and diluted appropriately prior to i.v. injection. Our frozen stocks contained negligible dead bacteria (96.88% viability, $p = 0.48$) compared with starting cultures for up to 5 months. FluoSpheres carboxylate-modified microspheres (yellow green, 1.0 μm) and Fluorescein-conjugated dextran (lysine-fixable, 70 kDa) were purchased from Invitrogen (Carlsbad, CA).

Histology

Spleens were harvested, embedded in OCT compound and 5 μm cryosections were prepared. Sections were fixed with 4% paraformaldehyde in PBS (pH 7.2) at 4°C for 5 min and blocked with StartingBlock Blocking Buffer (Thermo Fisher Scientific, Rockford, IL) for 10 min, then sequentially incubated with purified and/or biotin-conjugated primary antibodies and fluorescent-dye-conjugated secondary antibodies and/or fluorescent-dye-conjugated streptavidin. Antibodies and reagents used for staining were as follows: phalloidin-Alexa Fluor 350 (Invitrogen), rat anti-mouse F4/80 (biotin conjugated, BM8; eBioscience, San Diego, CA),

Rat anti-mouse/human CD45R/B220 (PE or Alexa Fluor 647 conjugated, RA3-6B2; eBioscience, or BD Biosciences, San Jose, CA), rat anti-mouse MARCO (PE-conjugated, ED31; Serotec, Oxford, UK), rat anti-mouse SIGN-R1 (biotin-conjugated, ER-TR9; BMA Biomedicals, Augst, Switzerland).

Rat anti-mouse siglec-1 (biotin or FITC-conjugated, MOMA-1; BMA Biomedicals or Serotec), hamster anti-mouse CD11c (biotin or PE-conjugated, HL3 or N418; BD Biosciences or eBioscience), rat anti-mouse CD11b (biotin, Alexa Fluor 647 or PE-conjugated, M1/70; BD Biosciences or eBioscience), rabbit anti-LM polyserum serotypes 1 and 4 (BD Diagnostic Systems, Sparks, MD), goat anti-rabbit IgG (FITC-conjugated; Sigma, St. Louis, MO), streptavidin (Alexa Fluor 555 or Alexa Fluor 647-conjugated; Invitrogen), rat anti-mouse Ly-6G(Gr-1) (PE-conjugated, RB6-8C5; eBioscience).

Immunofluorescence microscopy

Four-color fluorescence microscopy of cryosections was performed using an Olympus BX51 equipped with 100 W mercury lamp (Olympus America, Center Valley, PA) and a SPOT RT charge-coupled device camera (Diagnostic Instruments, Sterling Heights, MI). Monochrome images (1200 pi × 1600 pi = 885 × 1180 μm in 10× objectives; 440 × 586 μm in 20× objectives, 12-bit ;depth) were acquired with filter sets optimized for DAPI, FITC, tetramethyl rhodamine isothiocyanate (TRITC), and cyanine dye 5(y5, 670 nm emission), respectively (Chroma, Rockingham, VT). Exposure times of 1–2 s were used and a linear contrast stretch was applied to the images to normalize brightness. Monochrome images were pseudo-colored and merged into 24 bit RGB images with SPOT RT camera software and exported into Adobe Photoshop for subsequent color balancing and image segmentation. Colocalization coefficients and Pearson's correlation coefficients [33] were generated from pooled fluorescent images with Volocity software (version 3.7; Improvision, Waltham, MA). Color-balanced images were transferred to Volocity and RGB channels were split. Thresholds were set for each channel using automatic thresholding and were confirmed by eye; in cases where automatic thresholding failed, thresholds were re-adjusted manually comparable to other images. All data from three time points (30 min, 2 h, and 6 h) were first tested with One-way ANOVA (Kruskal–Wallis test, nonparametric). If the overall p-value was < 0.05, 30 min *versus* 2 h, and 30 min *versus* 6 h were secondarily tested with the Dunns test. $^*p<0.05$, $^{**}p<0.01$, $^{***}p<0.001$.

Acknowledgements: The authors thank Xin Zhang for the breeding and care of the mice used in this study and Bernd H. Zinselmeyer and Jennifer N. Lynch for helpful comments on the paper. The authors also thank Mary O'Riordan for providing the MORO-2 LM strain. This work was supported in part by a grant from the National Institutes of Health (AI062832, ERU).

Conflict of interest: The authors declare no financial or commercial conflict of interest.

References

1 **Junt, T., Scandella, E. and Ludewig, B.**, Form follows function: lymphoid tissue microarchitecture in antimicrobial immune defence. *Nat. Rev. Immunol.* 2008. **8**: 764–775.

2 **Khanna, K. M. and Lefrançois, L.**, Geography and plumbing control the T cell response to infection. *Immunol. Cell Biol.* 2008. **86**: 416–422.

3 **Kraal, G.**, Cells in the marginal zone of the spleen. *Int. Rev. Cytol.* 1992. **132**: 31–74.

4 **Mebius, R. E. and Kraal, G.**, Structure and function of the spleen. *Nat. Rev. Immunol.* 2005. **5**: 606–616.

5 **Elomaa, O., Kangas, M., Sahlberg, C., Tuukkanen, J., Sormunen, R., Liakka, A., Thesleff, I. et al.**, Cloning of a novel bacteria-binding receptor structurally related to scavenger receptors and expressed in a subset of macrophages. *Cell* 1995. **80**: 603–609.

6 **Sankala, M., Brannstrom, A., Schulthess, T., Bergmann, U., Morgunova, E., Engel, J., Tryggvason, K. and Pikkarainen, T.,** Characterization of recombinant soluble macrophage scavenger receptor MARCO. *J. Biol. Chem.* 2002. **277**: 33378–33385.

7 **Kang, Y. S., Yamazaki, S., Iyoda, T., Pack, M., Bruening, S.A., Kim, J. Y., Takahara, K. et al.,** SIGN-R1, a novel C-type lectin expressed by marginal zone macrophages in spleen, mediates uptake of the polysaccharide dextran. *Int. Immunol.* 2003. **15**: 177–186.

8 **Lanoue, A., Clatworthy, M. R., Smith, P., Green, S., Townsend, M. J., Jolin, H. E., Smith, K. G. et al.,** SIGN-R1 contributes to protection against lethal pneumococcal infection in mice. *J. Exp. Med.* 2004. **200**: 1383–1393.

9 **Kraal, G. and Janse, M.,** Marginal metallophilic cells of the mouse spleen identified by a monoclonal antibody. *Immunology* 1986. **58**: 665–669.

10 **Jones, C., Virji, M. and Crocker, P. R.,** Recognition of sialylated meningococcal lipopolysaccharide by siglecs expressed on myeloid cells leads to enhanced bacterial uptake. *Mol. Microbiol.* 2003. **49**: 1213–1225.

11 **Oetke, C., Kraal, G. and Crocker, P. R.,** The antigen recognized by MOMA-I is sialoadhesin. *Immunol. Lett.* 2006. **106**: 96–98.

12 **Crocker, P. R., Kelm, S., Dubois, C., Martin, B., McWilliam, A. S., Shotton, D. M., Paulson, J. C. and Gordon, S.,** Purification and properties of sialoadhesin, a sialic acid-binding receptor of murine tissue macrophages. *EMBO J.* 1991. **10**: 1661–1669.

13 **Eloranta, M. L. and Alm, G. V.,** Splenic marginal metallophilic macrophages and marginal zone macrophages are the major interferon-alpha/beta producers in mice upon intravenous challenge with herpes simplex virus. *Scand. J. Immunol.* 1999. **49**: 391–394.

14 **Jablonska, J., Dittmar, K. E., Kleinke, T., Buer, J. and Weiss, S.,** Essential role of CCL2 in clustering of splenic ERTR-9+macrophages during infection of BALB/c mice by *Listeria monocytogenes*. *Infect. Immun.* 2007. **75**: 462–470.

15 **Nathan, C.,** Neutrophils and immunity: challenges and opportunities. *Nat. Rev. Immunol.* 2006. **6**: 173–182.

16 **Conlan, J. W. and North, R. J.,** Neutrophils are essential for early anti-Listeria defense in the liver, but not in the spleen or peritoneal cavity, as revealed by a granulocyte-depleting monoclonal antibody. *J. Exp. Med.* 1994. **179**: 259–268.

17 **Czuprynski, C. J., Brown, J. F., Maroushek, N., Wagner, R. D. and Steinberg, H.,** Administration of anti-granulocyte mAb RB6-8C5 impairs the resistance of mice to *Listeria monocytogenes* infection. *J. Immunol.* 1994. **152**: 1836–1846.

18 **Rogers, H. W. and Unanue, E. R.,** Neutrophils are involved in acute, nonspecific resistance to *Listeria monocytogenes* in mice. *Infect. Immun.* 1993. **61**: 5090–5096.

19 **Unanue, E. R.,** Inter-relationship among macrophages, natural killer cells and neutrophils in early stages of Listeria resistance. *Curr. Opin. Immunol.* 1997. **9**: 35–43.

20 **Witmer, M. D. and Steinman, R. M.,** The anatomy of peripheral lymphoid organs with emphasis on accessory cells: light-microscopic immunocytochemical studies of mouse spleen, lymph node, and Peyer's patch. *Am. J. Anat.* 1984. **170**: 465–481.

21 **Dudziak, D., Kamphorst, A. O., Heidkamp, G. F., Buchholz, V. R., Trumpfheller, C., Yamazaki, S., Cheong, C. et al.,** Differential antigen processing by dendritic cell subsets in vivo. *Science* 2007. **315**: 107–111.

22 **Austyn, J. M. and Gordon, S.,** F4/80, a monoclonal antibody directed specifically against the mouse macrophage. *Eur. J. Immunol.* 1981. **11**: 805–815.

23 **Oldenborg, P. A., Zheleznyak, A., Fang, Y. F., Lagenaur, C. F., Gresham, H. D. and Lindberg, F. P.,** Role of CD47 as a marker of self on red blood cells. *Science* 2000. **288**: 2051–2054.

24 **Pamer, E. G.,** Immune responses to *Listeria monocytogenes*. *Nat. Rev. Immunol.* 2004. **4**: 812–823.

25 **Aichele, P., Zinke, J., Grode, L., Schwendener, R. A., Kaufmann, S. H. and Seiler, P.,** Macrophages of the splenic marginal zone are essential for trapping of blood-borne particulate antigen but dispensable for induction of specific T cell responses. *J. Immunol.* 2003. **171**: 1148–1155.

26 **Conlan, J. W.,** Early pathogenesis of *Listeria monocytogenes* infection in the mouse spleen. *J. Med. Microbiol.* 1996. **44**: 295–302.

27 **Muraille, E., Giannino, R., Guimalda, P., Leiner, I., Jung, S., Pamer, E. G. and Lauvau, G.,** Distinct in vivo dendritic cell activation by live versus killed *Listeria monocytogenes*. *Eur. J. Immunol.* 2005. **35**: 1463–1471.

28 **Neuenhahn, M., Kerksiek, K. M., Nauerth, M., Suhre, M. H., Schiemann, M., Gebhardt, F. E., Stemberger, C. et al.,** CD8alpha+dendritic cells are required for efficient entry of *Listeria monocytogenes* into the spleen. *Immunity* 2006. **25**: 619–630.

29 **Dijkstra, C. D., Van Vliet, E., Dopp, E. A., van der Lelij, A. A. and Kraal, G.,** Marginal zone macrophages identified by a monoclonal antibody: characterization of immuno- and enzyme-histochemical properties and functional capacities. *Immunology* 1985. **55**: 23–30.

30 **Metlay, J. P., Witmer-Pack, M. D., Agger, R., Crowley, M. T., Lawless, D. and Steinman, R. M.,** The distinct leukocyte integrins of mouse spleen dendritic cells as identified with new hamster monoclonal antibodies. *J. Exp. Med.* 1990. **171**: 1753–1771.

31 **Mitchell, J.,** Lymphocyte circulation in the spleen. Marginal zone bridging channels and their possible role in cell traffic. *Immunology* 1973. **24**: 93–107.

32 **Steinman, R. M., Pack, M. and Inaba, K.,** Dendritic cells in the T-cell areas of lymphoid organs. *Immunol. Rev.* 1997. **156**: 25–37.

33 **Manders, E. M. M., Verbeek, F. J. and Aten, J. A.,** Measurement of colocalization of objects in dual-color confocal images. *J. Microsc.-Oxford* 1993. **169**: 375–382.

34 **O'Riordan, M., Moors, M. A. and Portnoy, D. A.,** Listeria intracellular growth and virulence require host-derived lipoic acid. *Science* 2003. **302**: 462–464.

35 **Aoshi, T., Zinselmeyer, B. H., Konjufca, V., Lynch, J. N., Zhang, X., Koide, Y. and Miller, M. J.,** Bacterial entry to the splenic white pulp initiates antigen presentation to CD8+T cells. *Immunity* 2008. **29**: 476–486.

36 **Taylor, P. R., Martinez-Pomares, L., Stacey, M., Lin, H. H., Brown, G. D. and Gordon, S.,** Macrophage receptors and immune recognition. *Annu. Rev. Immunol.* 2005. **23**: 901–944.

37 **Nussenzweig, M. C., Steinman, R. M., Witmer, M. D. and Gutchinov, B.,** A monoclonal antibody specific for mouse dendritic cells. *Proc. Natl. Acad. Sci. USA* 1982. **79**: 161–165.

38 **Serbina, N. V., Salazar-Mather, T. P., Biron, C. A., Kuziel, W. A. and Pamer, E. G.,** TNF/iNOS-producing dendritic cells mediate innate immune defense against bacterial infection. *Immunity* 2003. **19**: 59–70.

39 **Tam, M. A. and Wick, M. J.,** Differential expansion, activation and effector functions of conventional and plasmacytoid dendritic cells in mouse tissues transiently infected with *Listeria monocytogenes*. *Cell. Microbiol.* 2006. **8**: 1172–1187.

40 **Arredouani, M., Yang, Z., Ning, Y., Qin, G., Soininen, R., Tryggvason, K. and Kobzik, L.,** The scavenger receptor MARCO is required for lung defense against pneumococcal pneumonia and inhaled particles. *J. Exp. Med.* 2004. **200**: 267–272.

